Dear author,

Please note that changes made in the online proofing system will be added to the article before publication but are not reflected in this PDF.

We also ask that this file not be used for submitting corrections.

CHAPTER 6

Colloidal Microfluidics

Max Meissner[1], Annela M. Seddon, C. Patrick Royall
[1]Corresponding author: e-mail address:

s0010 ## 6.1 Introduction

p0010 Colloidal science concerns itself with the study of particles or fluids suspended within other fluids. Found across all manner of industry, research, and biology, colloids and nanoparticles also possess qualities which allow them to act as model systems. Model systems greatly enhance our ability to interpret, understand, and investigate the universe [1, 2]. As a simplification or idealization of real-world phenomena, a scientific model aims to allow further insight and understanding of the much more complex phenomena it represents.

1

p0015 Models can of course be experimental, theoretical, or a combination of the two. An experimental model system attempts to capture some form of physical phenomenon in an idealized experimental system. One example of this is the simple pendulum. Ubiquitous in physics teaching laboratories, this experiment teaches undergraduate students that by understanding a simple system (the swinging pendulum) one can derive a broadly applicable mathematic relationship (simple harmonic motion) [1].

p0020 Colloidal particles offer a powerful experimental model system for research into a range of phenomena, from very small to very large systems. One example of this is the work carried out by Jean Perrin in the early 20th century, who showed that a dilute colloidal suspension of particles behaves much like an ideal gas [3]. The value of using colloidal particles as model systems stems from the fact that their interparticle interactions can be easily tuned allowing access to a wide parameter space. Additionally, due to the usual size of colloidal particles, they fall within a regime where their behavior is analogous to atomic systems, while still large enough to image via optical microscopy. In fact, this idea of considering colloidal particles as "big atoms" is fundamental to contemporary colloid science and provides insight into many diverse phenomena in the field of soft condensed matter [4].

p0025 The vast majority of colloidal model systems concern themselves with solid particles such as silica, polymethylmethacrylate, or comparable materials. While these are attractive options, an exciting alternative which is significantly less explored is the use of emulsions as model systems.

p0030 Emulsions are a subset of colloidal systems consisting of two or more immiscible liquids [5]. In an emulsion one liquid, known as the dispersed phase, is evenly distributed in the other liquid, known as the continuous phase. Emulsions are extremely common in industry, finding use as vinaigrettes, cosmetic creams, in oil extraction, paints, photographic film, and various other applications, including colloidal model systems. While the bulk of scientific literature concerns itself with the study of solid colloidal particles there is considerable interest in using emulsions as colloidal model systems.

p0035 The intrinsic softness of a system is an important consideration of model systems. While one of the most common model systems is the hard sphere approximation, in reality, colloidal particles always have a degree of "softness" [6]. By softness, in this case we refer either to interactions between particles which extend beyond the particle surface, often caused by high charges or polymer interactions, or to the deformability of the particle. This softness generally manifests as an increase in the effective volume fraction of the system, and thus is a powerful tool for adjusting the behavior of a particle suspension. However, softness also brings with it novel behaviors that cannot be found in harder particles. For example, in densely packed systems, softness of particles allows rearrangement of the particles facilitating higher packing fractions than would otherwise be possible.

p0040 Particle "softness" can be realized via several distinct methods, the first and the most common of these is electrostatics. These systems consist of conventional solid particles (often poly methyl methacrylate or silica) which have been imparted with a strong surface charge. The existence of this surface charge by necessity imparts upon the system a repulsion which decays with separation distance. Overall this has the effect of artificially increasing the effective volume of the particle and allows for a degree of "softness." Another plausible candidate for "soft" and deformable model systems is the microgel. Consisting of cross-linked polymer coils, a microgel swells depending on the solvent the particles are dispersed in, with sufficiently swollen microgel particles acting very "soft" indeed. Finally, emulsions can also act as "soft" model systems. Systems consisting of emulsions can easily rearrange themselves, with the "soft" interfaces of the droplet readily deforming themselves. However, unlike charged particles and microgels whose "soft" regions can readily compress, an emulsion must stay at a constant volume under any deformation. Due to this, emulsions lend themselves very well as a pseudo-hard sphere system in which the particles can rearrange, and freely flow past each other, but not overlap at high volume fractions [6].

p0045 A further advantage emulsions have is that most manufacturing methods allow for precise tuning of the system components, the stabilizing agents used, and the size of the particles. Thus, emulsions offer a versatile framework within which to develop model systems. Additionally, emulsions have molecularly smooth surfaces, avoiding any concerns of surface roughness, and entirely eliminating friction between particles [6]. Unfortunately, however, emulsions currently come with some challenges to their use as model systems. Emulsions tend to be rather polydisperse compared to solid particles and thus, in particular, study of systems involving crystallization is inhibited. Nevertheless, some promising examples of emulsion model systems to study gel formation have been reported [7–9].

p0050 Microemulsions are too small to study with real space imaging, high-pressure homogenization requires precision machined gratings and thus is very limited in the sizes it can be produced and is extremely expensive, high shear mixing tends to produce droplets with unacceptably broad size distributions. Chemical methods which allow for the direct synthesis of micron-scale droplets can produce monodisperse droplets of the appropriate sizes are excellent at producing large quantities of emulsions, however, they are limited to specific compositions [10]. One alternative to this is microfluidic emulsification, a relatively recent technique where emulsification occurs via highly controlled droplet breakup within a microchannel.

s0015 ## 6.2 Microfluidics

p0055 Microfluidics, at its simplest is the science and technology governing systems that manipulate small (10^{-9} L to 10^{-18} L) quantities of liquid in channels with dimensions smaller than a few hundred micrometers. Exploiting the high degree of confinement and the resulting non

turbulent laminar flow, microfluidic technologies offer fundamentally new capabilities for the control and analysis of low-volume samples [11]. Due to the significant reduction in sample quantity required, early applications of microfluidic technology have largely focused on analytical techniques.

p0060 In particular due to the staggering decrease in analytical cost, coupled with high sensitivity, speed, and low sample volumes, microfluidic techniques have rapidly gained applications in the field of medical and life sciences research. Some key applications include in situ separation prior to mass spectroscopy [12], high-throughput drug screening [13], single cell manipulation [14], nano-liter chemical synthesis [15], time resolved reaction kinetics [16], and multiphase flows [17].

p0065 The history of microfluidics dates back as far as the mid-1950s where the development of ink jet printers spurred research in the field of droplet production and handling [18]. A few decades later, inspired by Richard Feynman's "There's plenty of room at the bottom" address [19], some preliminary research into biosensing and medical sciences applications began [20]. However, the miniaturization of fluidic components could not keep pace with the microelectromechanical systems of the time, and thus research interest in fluidic systems waned.

p0070 In the 1980s, however, microfluidics research was re-invigorated by innovations in microlithography. For the first time, truly "micro" systems were within reach. These devices were rapidly used for applications such as automotive gas sensors, particle sorting, and guided assembly. However, as these methods relied on costly and time-consuming lithographic techniques, the scope of this research remained somewhat limited.

p0075 The field of microfluidics as we know it today, focusing on rapid prototyping and disposable single-use devices, first came into being in the late 1990s. At this time, the Whitesides group pioneered soft lithography [21], a process where polydimethylsiloxane (PDMS) stamps were produced to transfer complex patterns for lithography. Shortly after, this method was shown to be a versatile system for fully enclosed microfluidic channels, allowing rapid prototyping of high-quality microchannels [21]. Following this, the Quake group at Stanford utilized these methods for highly complex microfluidic valve systems [22]. These innovations for the first time brought microfluidics to the masses. The vast reduction in cost and manufacturing complexity brought to bear here, allowed the field of microfluidics research to rapidly expand. Today, over 3000 papers a year are published on the topic of microfluidics, and microfluidic technologies have spawned global industries worth over \$2.5 billion a year, with double digit year on year growth.

p0080 These modern microfluidic systems come in a huge range of shapes and sizes, although the vast majority are composed of PDMS. Finding applications as varied as cellular diagnostics or miniaturized reaction vessels, these devices have opened new avenues of research across just

about all areas of the experimental sciences. Microfluidic emulsification in particular has found a vast number of potential applications. However, despite the many advantages microfluidics offers in the field of soft matter, microfluidic emulsification has not found much use in colloid science [23].

s0020 6.3 Basic Principles of Microfluidic Flow

s0025 6.3.1 Navier–Stokes Equation

p0085 Broadly speaking the behavior of microscale flows differs significantly from macroscopic flows. Otherwise useful mathematical descriptors of fluid motion such as Euler's equation or the Bernoulli equations, due to fact they ignore viscous effects, become largely irrelevant on the microscale. Instead one needs to use the Navier–Stokes equation to describe fluid flow on the relevant size scales. Named after two titans of fluid dynamics: Claude-Louis Navier and George Gabriel Stokes, the Navier–Stokes equations describe the motion of viscous fluids. While the Navier–Stokes equations can be used to describe all manner of fluids, the form most relevant for microscale liquid flow is the equation for the case of a noncompressible fluid:

$$\rho\left(\frac{\partial v}{\partial t}+v\cdot\nabla v\right)=-\nabla p+u\nabla^2v+f \tag{1}$$

p0090 However, at the micrometer length scales commonly found in microfluidic systems, the inertial force terms becomes negligibly small and the equation can reduce down to a condensed form:

$$\nabla p=u\nabla^2v \tag{2}$$

p0095 This simplified noninertial Navier–Stokes equation allows us to begin understanding microfluidic flow. From this equation we can extract that the pressure drop is proportional to the viscosity multiplied by the second derivative of the fluid velocity. However, even in this reduced form, the Navier–Stokes equation remains challenging for use with any practical applications of fluid flow, and directly solving these equations remains firmly in the domain of computational fluid dynamics. Instead, much of a fluidic system's behavior can be inferred via the use of dimensionless parameters.

s0030 6.3.2 Dimensionless Parameters in Microfluidic Flows

p0100 As in any fluidic system, the broad behavior of the fluid can be described by a myriad of dimensionless parameters. Relating the relative importance of various competing phenomena, these dimensionless parameters provide a powerful lens with which to critically analyze the behavior of a fluid. Of these dimensionless parameters, the ones of key importance are the Reynolds number, Re, the Péclet number, Pe, the capillary number, Ca, and for multiphase flow

6   Chapter 6

the Weber number, *We*. These dimensionless parameters serve to, if not exhaustively explain, at least qualitatively describe the behavior of fluid flow in microfluidics and where it differs from larger scale, less confined flows.

s0035 ### 6.3.2.1 Reynolds Number

p0105 Of all the dimensionless parameters that govern fluid flow, when it comes to microfluidics, the Reynolds number is often described as one of the most defining parameters. Counter intuitively, however, the Reynolds number is arguably also the least useful in describing microfluidic systems. The Reynolds number, $Re = f_i/f_v$, relates the relative magnitude of inertial forces to viscous forces, and is commonly expressed as:

$$Re = \frac{\rho v L}{\mu} \tag{3}$$

p0110 where ρ is the fluid density, L is a characteristic length scale of the system, and μ is the fluid viscosity. The magnitude of the Reynolds number provides a powerful insight as to whether fluid flow will be turbulent or laminar.

p0115 Where Reynolds numbers are very small, usually $Re \ll 100$, inertial forces are dominated by viscous forces, the nonlinear inertial term of the Navier–Stokes equation drops off, and the fluid flow becomes a linear and predictable laminar flow. As the Reynolds number increases, the first effects of turbulence may appear at Reynolds numbers of around 1000, however, this can happen earlier in curved pipes where centrifugal forces can give rise to a secondary "Dean flow." As the Reynolds number gets even higher, the nonlinear inertial term of the Navier–Stokes equation destabilizes the flow resulting in unpredictable turbulent flow. The best example of this is Reynolds' experiments from 1883, where fluid dye inserted into a fluid flowing through a circular pipe was observed (Fig. 1). At Reynolds numbers above a critical, or transitional, Reynolds number (usually on order of $Re \gtrsim 2000$) fluid flow will tend to be turbulent. Flows between $Re \gtrsim 2000$ and $Re \gtrsim 1000$ can be either turbulent or laminar. Finally flows where $Re < 1000$ tend to be laminar.

Laminar flow

Turbulent flow
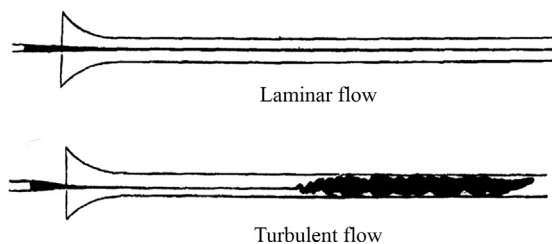
Fig. 1

f0010 Diagram from Reynolds 1883 paper illustrating the difference in flow of a fluid through a pipe. At low Reynolds numbers the dye remains a narrow tendril now mixing with the bulk fluid. At high Reynolds numbers, however, the flow becomes turbulent and the dye rapidly mixes with the carrier fluid.

p0120 In a microfluidic system, due to the characteristic micron-sized length scale, the Reynolds number is generally very small, with $Re < 10$. This of course implies that in a confined microfluidic system flow is almost entirely viscosity driven preventing turbulent flow. Without the inertial nonlinearity present in larger scale flows, inertia rarely plays a role in microfluidic systems, and microfluidic flows are straightforward and deterministic, an effect which gets more and more pronounced the smaller microfluidic systems become. It is precisely due to this absence of inertial nonlinearity that the Reynolds number becomes one of the key factors differentiating microfluidic flow from larger scale systems, while at the same time, providing very little detailed information about the flow in a microfluidic system.

s0040 ### 6.3.2.2 Péclet Number

p0125 While the Reynolds number drops in significance as the scale of a system decreases, there are many physical processes that become more complex and relevant as the system size decreases. One of these is diffusion: in a high Re environment, turbulent mixing enhances concentration gradients and reduces the time scale for mixing. Generally purely diffusive mixing has a very small net effect on the rate of mixing, when compared to this turbulent mixing. When considering smaller length scales, however, Re is small and turbulent mixing is suppressed, forcing mixing to occur via diffusion alone. Thus the next dimensionless parameter to be examined is the Péclet number. This dimensionless parameter concerns the diffusion of a system. While for colloidal particles, this is often compared to the sedimentation of a particle, in this context we use the Péclet number to compare diffusion and convection in a fluid, for example, for fluid moving down a micro-channel:

$$Pe = \frac{U_a H}{D} \tag{4}$$

where U_a is the fluid velocity, H is a characteristic channel dimension perpendicular to the direction of fluid flow, and D is the coefficient of diffusion of the particle or molecule of interest. Much like the Reynolds number, we can see that on the length scales commonly found in microfluidic systems $Pé$ will need to be very large to ensure complete mixing. In practice, in systems with low values of $Pé$, it will be extremely challenging to get two flows to thoroughly mix. The species of interest are much more likely to remain on the trajectory of the fluid flow, than to migrate across a channel. However, when one considers microfluidic devices in which the geometry and length scales have been carefully chosen to allow intermediate Péclet numbers, this phenomenon can be utilized as the foundation of several clever applications. Among these many applications, one example is T-sensors shown in Fig. 2, these are a system in which two fluids are brought into contact in a T-junction, flowing down the center alongside each other. Solute molecules in each stream diffuse into the other forming an interdiffusion zone which can be measured with a fluorescent marker. These T-sensors can be used to measure solute concentration [24] or probe diffusion kinetics [25].
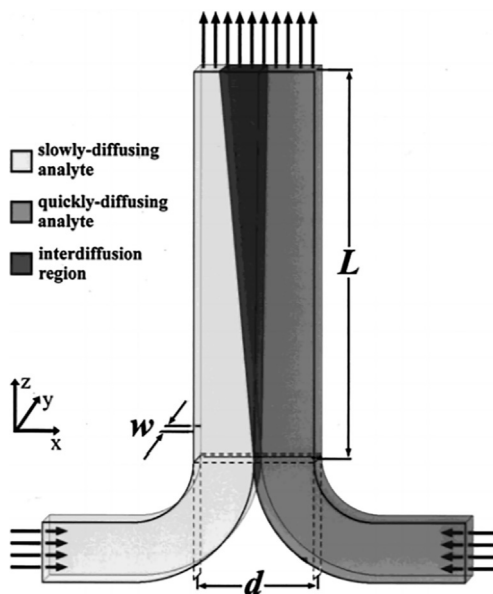
Fig. 2

f0015   Schematic of a T-sensor microfluidic device with two input fluids, each containing one diffusive species. The flow is steady state, and the asymmetric development of the interdiffusion region is a result of the difference in diffusion coefficients. *Reprinted with permission from A.E. Kamholz, B.H. Weigl, B.A. Finlayson, P. Yager, Quantitative analysis of molecular interaction in a microfluidic channel: the T-sensor, Anal. Chem. 71 (23) (1999) 5340–5347, ISSN 00032700,* https://doi.org/10.1021/ac990504j. *Copyright 1990 American Chemical Society.*

s0045   ### 6.3.2.3 Capillary Number

p0130   While in the above sections we have assumed that the fluids of interested are miscible, in the context of droplet generation we must now examine dimensionless parameters relevant for immiscible fluids. The key difference in these systems is of course that between two immiscible fluids, there exists an interface, and a surface tension, γ. This surface tension is definitive in the behavior of immiscible phase, multiphase microfluidics. As such, the next dimensionless parameter to be examined is the capillary number:

$$Ca = \frac{\eta U_0}{\gamma} \tag{5}$$

where η is the outer phase fluid viscosity, U_0 is the outer phase fluid velocity, and γ is the surface tension between the two immiscible fluids. This capillary number is relevant whenever one finds a system with competition between interfacial and viscous stresses. In particular, the capillary number is exceedingly relevant in any system which aims to produce droplets via microfluidic means. In a droplet producing system, the two immiscible fluids are brought into contact and an interface arises, as the interface gets dragged in the direction of flow, the

interface stretches out and the surface tension is forced to compete with the viscous drag in attempting to minimize the surface area. These competing stresses cause the interface to destabilize, and are the main mechanism governing the behavior of droplet microfluidics.

s0050 ### 6.3.2.4 Weber Number

p0135 While generally the capillary number is of paramount importance due to the low relevance of inertia, in certain flow regimes inertia can occasionally play a role. To examine systems such as these, one needs to consider a dimensionless parameter which relates the inertia of a multiphase system to the surface tension between the fluid phases, this is the Weber number:

$$We = \frac{\rho v^2 l}{\sigma} \tag{6}$$

where ρ is the density of the fluid, v is the velocity of the fluid, l is a characteristic length scale, usually the diameter of the droplet or bubble, and σ is the surface tension. This dimensionless parameter is of particular interest when considering the deformation of droplets. As such it finds relevance particularly in droplet manipulation or splitting devices, for example, in T-junction droplet splitters.

s0055 ### 6.3.2.5 Dimensionless Number Summary

p0140 Please see Table 1.

s0060 ## 6.4 Microfluidic Devices

p0145 Early microfluidics were often extremely crude systems, relying on simple etched channels or micromachined silicon. Since these early days, however, advancements in materials technology and manufacturing methods have significantly increased the variety of devices available. Devices today can include features of almost any geometry at extremely high feature resolutions, across a wide range of materials.

s0065 ### 6.4.1 Materials

p0150 The first consideration when designing microfluidics is of course the material choice. For this, one must consider the material requirements for the system in question, as well as the complexity and cost. For low-cost microfluidics, one attractive option currently available is paper microfluidics. These devices usually consist of a wax or silicone layer on a paper

t0010   **Table 1: Table of relevant dimensionless numbers for microfluidic flows.**

Re	Reynolds	$\rho v L / \mu$	Inertial/viscous	Eq. (3)
Pe	Péclet	$\frac{U_a H}{D}$	Convection/diffusion	Eq. (4)
Ca	Capillary	$\frac{\mu U_0}{\gamma}$	Viscous/interfacial	Eq. (5)
We	Weber	$\frac{\rho v^2 l}{\sigma}$	Inertial/interfacial	Eq. (6)

substrate. The device channels are etched into this wax or silicone layer, allowing for rapid and low-cost manufacture of even complex devices. However, the minimum size of microfluidic features is rather larger than alternative methods, and additionally, due to obvious technical constraints, these devices tend to be less robust than alternative methods [26–28]. A further consideration is chemical compatibility.

p0155 For simple systems involving aqueous or otherwise "benign" components, the choice of material is less relevant. However, for systems that involve powerful solvents, or chemically active species, more robust materials need to be used. For extremely aggressive liquids one can use devices directly etched into silicon or glass. These devices, however, are rather difficult to manufacture and thus can be prohibitively costly [29]. A similarly effective option is to manufacture devices out of resilient polymers [30] or Norland optical adhesives, a fast curing UV polymer with excellent chemical compatibility [31]. This choice of materials is also of relevance when it comes to the surface properties of multiphase microfluidic systems, where care must be taken to optimize the surface properties to ensure suitable flow conditions.

s0070 ## 6.4.2 Manufacturing Methods

p0160 Far removed from the painstaking early days of microfluidic manufacture, modern microfluidic manufacturing methods range from mechanically simple techniques such as scribing channels straight onto a glass slide to highly complex methods such as three-dimensional (3D) printing.

s0075 ### 6.4.2.1 Glass Capillary Microfluidics

p0165 By far the simplest microfluidic devices available, glass capillary devices are commonly used for droplet generation. In a glass capillary device the droplet phase is inserted through a narrow glass capillary into a larger chamber containing the continuous fluid, either stationary or flowing. This continuous phase can be contained either in a conventional microfluidic device or within a second larger capillary. More complex realizations of this technology include concentric multilayered capillary for three-component flow focusing [32].

s0080 ### 6.4.2.2 Micromachining

p0170 Silicon micromachining is a widely used technique in the manufacture of microelectromechanical systems, and was one of the earliest manufacturing techniques applied to microfluidics. While this technique does offer high-resolution patterning, silicon is often a less than ideal material for microfluidics. The rigidity, optical properties, high cost, and surface properties of patterned silicon make it hard to integrate these chips with flow components, and make applications for biological purposes challenging. However, due to the robustness of silicon devices, this technique still finds use in applications that require highly stable surface chemistry, high-temperature compatibility, or excellent chemical compatibility [33].

6.4.2.3 Soft Lithography

p0175 In order to foster further development of microfluidic devices, a fast, cheaper, and more versatile method than the methods described above was required. Soft lithography proved to be the solution, and the current prevalence of microfluidic methods largely owes its success to this method. First developed in 1974, as elastomeric micromolding by Bell labs, this method involved molding a soft material using a lithographic master [34]. Since then, the concept of soft lithography has been used to pattern all manner of surfaces via stamping and hot embossing. The first practical demonstrations of this technique came around in the 1980s, where Masuda et al. demonstrated a microfluidic circuit capable of performing complex operations on living cells [35].

p0180 It was not until the late 1990s, however, that Whitesides et al. demonstrated their method of using PDMS as a device material molded directly onto photo-lithography produced molds [36]. In this method, as the polymer is cured directly on the device pattern itself, the resolution and complexity of the produced devices therefore is dependent only on the quality of the lithographic process, and the mechanical properties of the polymer.

p0185 Alternative soft lithographic methods for device fabrication can include methods such as hot embossing. Hot embossing refers to transferring a pattern from a micromachined metal master to a pliable plastic substrate. By heating the master and applying it to a plastic surface at high pressure this method imprints the master pattern onto the plastic substrate. The advantage of this method is, due to the rapid embossing speed and high reproducibility, that hot embossing can be used to mass produce devices at low cost. However, as the master must be micromachined for this, the resolution is limited and any change in the pattern requires essentially starting over with a new design [37].

s0090 ## 6.4.2.4 Micromolding

p0190 Injection molding is a powerful established technique for low-cost, high-throughput fabrication of microfluidic devices [38]. Just like conventional microinjection molding, here a thermoplastic polymer is heated past its glass transition temperature until soft and pliable. The hot polymer is then injected into a cavity that contains the device master, as the master is kept at a lower temperature than the plastic, rapid cooling occurs and the molded part is ready within just a few minutes. However, much like hot embossing, manufacture of the master is both time consuming and expensive. Conventionally this master is manufactured using methods such as micromachining or electroplating. While micromolding shares the same problems of cost and complexity as master as hot embossing, micromolding is a far faster technique and is thus the preferred method for mass production, even if the final microfluidic chips are of significantly lower resolution than is possible with soft lithography.

s0095 *6.4.2.5 3D Printing*

p0195 A relative newcomer to the field of microfluidic manufacturing, 3D printing holds great promise for rapid prototyping of microfluidic devices. The advantages of 3D printing for microfluidic applications are manifold, first, the speed of 3D printing compares favorably to the alternative methods detailed above. This of course allows far faster incrementation and prototyping allowing a much larger range of devices to be tested and implemented. Second, unlike lithographic methods, which are largely limited to planar geometries, 3D printing allows the production of truly 3D devices, allowing complex multilayer devices to be produced with greater ease than any comparable methods [39].

p0200 While early attempts at 3D printing microfluidics ultimately proved futile due to the resolution limits of early printers, modern techniques are far more suitable for microfluidic applications. In recent years the steadily decreasing cost and increased availability of 3D printing technologies such as stereo-lithography or two-photon polymerization have opened up the field of microfluidics to impressive applications of 3D printing technologies. With products such as the Nanoscribe 3D printer, the dream of directly manufacturing device features in situ with micron-scale resolution is rapidly becoming reality [40].

s0100 **6.4.3 Microfluidic Device Features**

p0205 When taking into account both the variety of materials available, and the possible manufacturing methods one can use, the range of potential devices can quickly seem overwhelming. However, through careful consideration of the required parameters one can quickly eliminate unsuitable combinations. For example, for larger devices without complex geometries, 3D printing microfluidic devices would likely be the optimal choice. On the other hand, smaller, more complex devices require photo-lithography in order to achieve the required resolution. Overall, however, while obviously the availability of manufacturing techniques and materials does constrain the possible device designs, any microfluidic devices share several main design features, and device designs optimized for one method may well work for a variety of applications.

s0105 *6.4.3.1 Channel Dimensions*

p0210 While often limited by the manufacturing methods available, the channel dimensions are nonetheless an important consideration when designing a microfluidic device. In order to examine these parameters more closely, we must first consider the case of flow resistance in a microchannel. The flow rate within a microchannel is given by $Q = \Delta P/R$ where Q is the volumetric flow rate, ΔP is the pressure drop across the channel, and R is the channel resistance. This flow resistance is strongly dependent on both the channel shape and the aspect ratio of the channels themselves. For fluid flow in a channel with a circular cross section, the fluid resistance can be calculated using Eq. (7):

$$R = \frac{8\mu L}{\pi r^4} \tag{7}$$

p0215 where μ is the velocity of the fluid, L is the channel length, and r is the radius of the channel. While for a rectangular microchannel with a low aspect ratio (in systems where the width of the channel is close to the height), the flow resistance must instead be calculated using Eq. (8):

$$R = \frac{12\mu L}{wh^3}\left[1 - \frac{h}{w}\left(\frac{192}{\pi^5}\sum_{n=1,3,5}^{\infty}\frac{1}{n^5}\tanh\left(\frac{n\pi W}{2h}\right)\right)\right]^{-1} \tag{8}$$

p0220 where w is the channel width and h is the channel height. Finally, the flow resistance of a rectangular microchannel with a high aspect ratio can be found by Eq. (8):

$$R = \frac{12\mu L}{wh^3} \tag{9}$$

p0225 In addition to playing a crucial role in the flow resistance of a microfluidic device, the aspect ratio is also important from a material point of view. If a soft material such as PDMS is used the aspect ratio of the channels becomes a crucial consideration. If the aspect ratio is too low, a situation which can easily occur when designing pillars or similar obstructions, the material can bend and deform, preventing the geometry from carrying out its intended role. On the other hand an aspect ratio that is too high, with channels far wider than they are deep, will likely droop or sag obstructing the channel and inhibiting stable flow.

p0230 Providing a significant contribution to the flow resistance, the cross-sectional shape of the channel is also relevant to the distribution of flow in the channel. Due to the no-slip boundary conditions found at the interface between fluid and channel, we can expect a circular channel to have rotationally symmetric flow profiles. Rectangular channels on the other hand will have an asymmetric fluid flow profile, and in particular, there can be large differences in fluid velocities in the corners of the channel.

s0110 ### 6.4.3.2 Micromixers

p0235 Another common microfluidic feature is a mixing geometry. Mixing is an essential process required for many biological and chemical applications. However, the laminar conditions at the low Reynolds numbers commonly found in microfluidic systems prevent nondiffusive mixing. However, diffusion simply does not occur fast enough to provide adequate mixing for most applications. In order to overcome this, often complex device geometries must be used in order to induce mixing. In a microfluidic system, there are two primary methods for mixing multiple fluid flows together. Firstly there are passive mixers. These utilize complex channel geometries to fold fluids over themselves, increasing the contact area between flows, thereby increasing the rate of diffusion.

p0240 These micromixers offer a few key advantages, primarily in terms of manufacturing. As geometric features, these mixers can simply be incorporated into conventional planar microfluidic devices with very little modification required. Passive mixing can occur via a range of different geometries, the of which is a *y*-type geometry. In this geometry, the two fluids to be mixed are simply brought into contact in a *y*-junction, and are forced through a long channel allowing mixing to proceed via diffusion alone. This method, however, is less useful for more viscous flows or flow systems with very low Reynolds numbers [41].

p0245 A slightly more complex method which is more suitable for lower Reynolds numbers, is the split and recombine method of passive mixing. Here the two fluids are first brought into contact in a generic geometry, thus forming a laminar flow. This laminar flow is then repeatedly moved past flow splitting geometries, repeatedly splitting and rejoining the fluid, each time generating a new interface across which diffusion can occur [42].

p0250 An alternative method, similar to the split and recombine method, is the multi laminating mixer. In this geometry multiple alternating fluid tendrils are inserted into a fluid channel, generating multiple fluid interfaces. One of example of this is a cyclone mixer shown in Fig. 3, here the mixing fluids are inserted into a large circular chamber with a single central outflow. The laminar fluid threads spiral around this outflow significantly increasing the rate of diffusion and thus, mixing efficiency [43].

p0255 Finally, another common method of passive mixing is the serpentine microchannel. These device features rely on the phenomenon that "twisted pipe" geometries can enhance mixing even at low Reynolds numbers [44]. This mixing enhancement arises due to chaotic advection, in which simple velocity fields have been shown to produce chaotic particle trajectories. Manifesting as rapid distortion and elongation of interfaces between fluids, this significantly increases the contact area between two fluids enhancing diffusive mixing. While this method is used to great effect on the macroscale, microfluidic implementations have demonstrated similar effectiveness. In these devices, complex repeating 3D channels are produced with multilayer soft lithography. The mixing fluids are brought together, and then forced through multiple repeated right angle turns arranged in a helical manner. One example of this, demonstrated by Lie et al. allowed mixing of two fluids on timescales 100 times shorter than purely diffusive mixing [45].

p0260 While passive mixers are certainly attractive in terms of cost and ease of manufacturing, systems with very low Reynolds numbers remain challenging to sufficiently mix. Thus, an alternative for microfluidic mixing is the active mixer. These active mixers, often requiring moving parts or carefully aligned field inducers, are obviously significantly more complex mechanically than the passive mixers described above. Nevertheless, because they use an external energy source to mix the fluids, rather than relying solely on the fluid flow, active mixers can be used in systems otherwise too small or viscous for passive mixing.
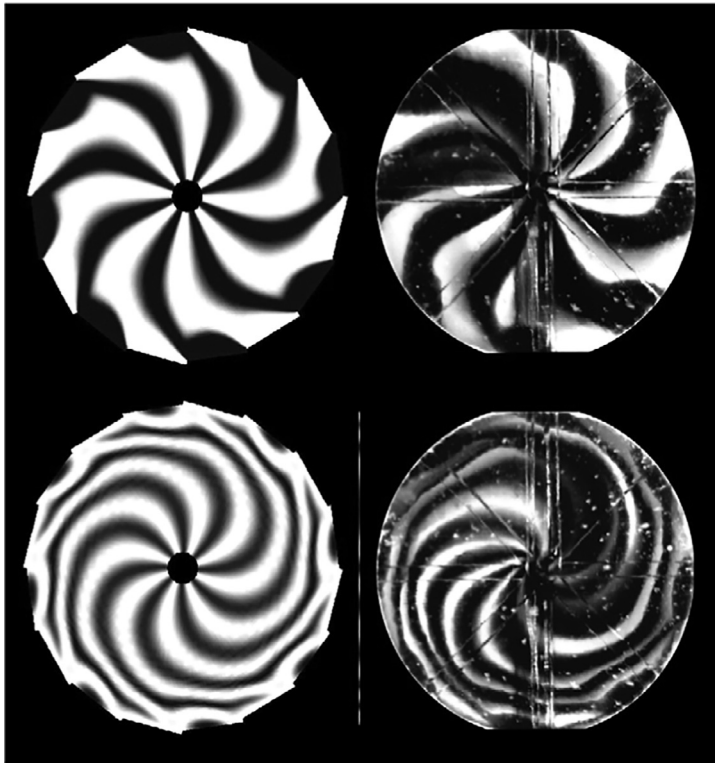
Fig. 3

f0020 Microscopy image of cyclone micromixer showing effective mixing of multiple fluids in a circular microchamber. *Reproduced from S. Hardt, T. Dietrich, A. Freitag, V. Hessel, H. Löwe, C. Hofmann, A. Oroskar, F. Schönfeld, K.M. Vanden Bussche, Radial and tangential injection of liquid/liquid and gas/liquid streams and focusing thereof in a special cyclone mixer, in: Sixth International Conference on Microreaction Technology, IMRET, vol. 6, 2002, pp. 329–344.*

p0265 The simplest method of active mixing is flow pulsation which involves periodically switching the flow rates between the two fluids being mixed. This pulsation of the flow distorts in the interface into an asymmetrically curved shape which distorts further over time. This distortion one again increases the effective surface area across which diffusion can occur and enhances mixing. Another method of active mixing involves utilizing ultrasonic fields generated by piezoelectric transducers as demonstrated by Yang et al. these piezoelectric membranes operating in the kHz range allow the formation of turbulent eddies facilitating mixing [46].

p0270 Finally, a very powerful but technically complex method of mixing is the microimpeller. Commonly used on the macroscale, impeller mixing is an extremely powerful mixing method, but requires complex rotating parts difficult to manufacture on the microscale. However, by taking advantage high-resolution etching of a ferromagnetic alloy Lu et al. demonstrated a 10-μ m scale micromixer capable of mixing at 600 rpm [47].

s0115   6.4.3.3 3D Devices

p0275 Briefly touched upon in Section 6.4.2.5, one avenue of microfluidics with tremendous potential is 3D devices. Due to the constraints of the commonly used lithographic techniques, the vast majority of microfluidic devices are planar in nature. However, with careful alignment of multiple PDMS devices or direct 3D printing of the channels it is possible to generate devices in which the channels incorporate 3D features. These features can be highly complex such as multilayer interwoven channels for mixing [48]. Alternatively, in the context of droplet microfluidics, 3D devices allow the generation of droplets via step emulsification. Step emulsification is a powerful emulsification technique which starts out much like a normal microfluidic device. The continuous fluid and droplet fluid coflow in a quasi two-dimensional Hele-Shaw flow regime. Once a stable flow is established, and a tendril of the droplet phase is completely engulfed by the continuous phase, the coflowing system is passed over a sudden deepening of the channel. This abrupt transitions and loss of confinement leads to the formation of highly uniform droplets [49]. A key advantage of this technique is that step emulsification lends itself well to parallel operation, facilitating high-volume production, a factor that makes this technique very well suited for lab on a chip applications [50].

s0120   6.4.3.4 Connectors and Resistors

p0280 A further universal feature of microfluidic systems are the inlets/outlets that serve to deliver and remove fluid from the system. While at first this may seem straight forward, in practice these structures often prove to be problematic due the vastly larger size of connecting tubing than the device features. Requiring aspect ratios far below what the material can sustain, these device features require complex patterns of reinforcing structures such as pillars. Secondly these features must allow sufficient fluid flux to enter the system, while also gradually reducing the flow rate sufficiently to avoid damaging the channels. In order to ensure uniform and stable flow, these inlets can incorporate filters. Simply including a repeating pattern of pillars is usually sufficient for this, and will serve to strain out any undesirable particulates. Often directly coupled to fluid inlet or outlets, are fluid flow resistors. These device features, often taking the form of serpentine channels serve to both adjust the pressure drop across a device and act as a damping mechanism to reduce the effects of pressure or flow fluctuations in the fluid flowing through the channel.

s0125   6.5 Microfluidic Manufacture

s0130   6.5.1 PDMS Microfluidics

p0285 Introduced in 1998 by Whitesides et al. [21] the rapid prototyping of microfluidic channels using PDMS has rapidly become the standard method of manufacturing microfluidic devices. The defining characteristic of PDMS allowing its prevalence in the microfluidic world is the high accuracy and rate of rapid prototyping structures. By utilizing the speed of conventional

photolithographic techniques as the templating method, PDMS devices can be produced extremely rapidly with minimal feature and pattern loss.

p0290 Prior to the introduction of the Whitesides PDMS rapid prototyping method, microfluidic fabrication was dependent on directly mechanically etching microfluidic channels into glass or quartz. PDMS reproduction of photolithographic channels was demonstrated to offer micron-scale manufacturing accuracy at significantly lower cost than mechanical etching. Alongside this, PDMS offers significant ease of assembly, as plasma oxidation allows for facile sealing of microfluidic channels. Finally, due to the chemical inertness and biocompatibility of PDMS, coupled with its low-cost PDMS was vastly more suitable for biological applications than previous iterations of microfluidic systems. Taking all of these advantages into account, PDMS has rapidly become the "gold-standard" of microfluidic materials. In particular, PDMS microfluidics has led to explosion of the lab-on-a-chip field. The low-sample volumes required, coupled with the low-cost of PDMS allows for highly sensitive, low-cost medical devices to be easily manufactured.

s0135 ## 6.5.2 PDMS Properties

p0295 PDMS owes its wide adoption in industrial applications to its favorable physical and chemical properties: PDMS is optically clear, inert, nontoxic, and inflammable. Additionally, these physical properties can be carefully tuned by adjusting the synthetic parameters, the cross-linking methods, and the curing times.

s0140 ### 6.5.2.1 Chemical Structure and Synthesis

p0300 Made up of repeating dimethylsiloxane monomers, PDMS is most commonly found as a viscoelastic silicone oil. PDMS is commonly synthesized via a polymerization reaction involving dimethyldichlorosilane. The reaction is as follows:

$$n\text{Si}(\text{CH}_3)_2\text{Cl}_2 + (n+1)\text{H}_2\text{O} \rightarrow \text{HO}[-\text{Si}(\text{CH}_3)_2\text{O}-]_n\text{H} + 2\,n\text{HCl}$$
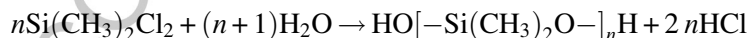
p0305 Through careful postprocessing of the PDMS polymers obtained via the reaction above, PDMS can be manufactured in a range of viscosities, from freely flowing oils to thick semisolid variations. Due to the siloxane linkages between monomers, PDMS molecules have relatively flexible backbones or chains, giving PDMS unusually high viscoelasticity; and these flexible chains can become loosely entangled at high polymer molecular weights, increasing the viscoelasticity (Fig. 4).

s0145 ### 6.5.2.2 Cross-Linking

p0310 While finding many applications an oil PDMS can also be cross-linked into a solid elastomeric material. This cross-linking can differ subtly from manufacturer to manufacturer, however, the most common methods involve an addition cure mechanism. An addition curing system obtains its name from the addition reaction with which the polymer is built. With this method of
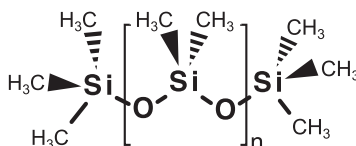
Fig. 4

f0025   Chemical structure of polydimethylsiloxane polymer backbone.

curing, a catalyst is added to a mixture of two polymer components. Most commonly in the case of silicones this catalyst is a platinum or peroxide catalyst. The two components consisting of a silicone hydride and a silicon vinyl then undergo a catalyzed addition reaction, forming an ethyl bridge between the monomer units. One advantage of this system is that the addition reaction does not form any by-products significantly reducing the risk of chemical contamination. After mixing, this curing is drastically accelerated by heat treatment, with temperatures of around 100°C reducing the time required for the elastomer to solidify by an order of magnitude.

p0315 Overall, addition curing as a method of cross-linking results in a sturdy elastic polymer with excellent mechanical and chemical resiliency. This in situ curing allows almost perfect pattern replication when cured on a transfer pattern or mold, allowing accurate replication of even micron-scale structures. Coupled with the elastomeric, chemical, biocompatible, and optical properties of PDMS, this ease of pattern replication allowed PDMS to become the material of choice for microfluidics.

s0150 ### 6.5.2.3 Optical Properties

p0320 PDMS has ideal optical properties for most forms of optical microscopy, which contributes immensely to the adoption of PDMS as a tool for in situ analysis. The high transparency of PDMS coupled with low absorbance of common fluorescence wavelengths allows imaging of samples to be carried out directly within PDMS microchannels. Additionally, PDMS has found some use in the manufacture of photonic components: the ease with which additives such as fluorophores or nanoparticles can be embedded in PDMS allows careful tuning of the optical properties of the material [51, 52].

s0155 ## 6.5.3 Manufacturing Microfluidics

p0325 Due its versatility the manufacture of PDMS microfluidic devices can proceed via a large range of different routes, including direct molding of PDMS on patterns, spin coating of PDMS onto patterned substrates, or using PDMS to stamp lithographic features onto substrates. However, overwhelmingly the manufacturing method used is the method introduced by the Whitesides group as schematically represented in Fig. 5. This method involves producing a lithographic template, curing PDMS on the template, and finally plasma bonding PDMS to seal the microfluidic channels.
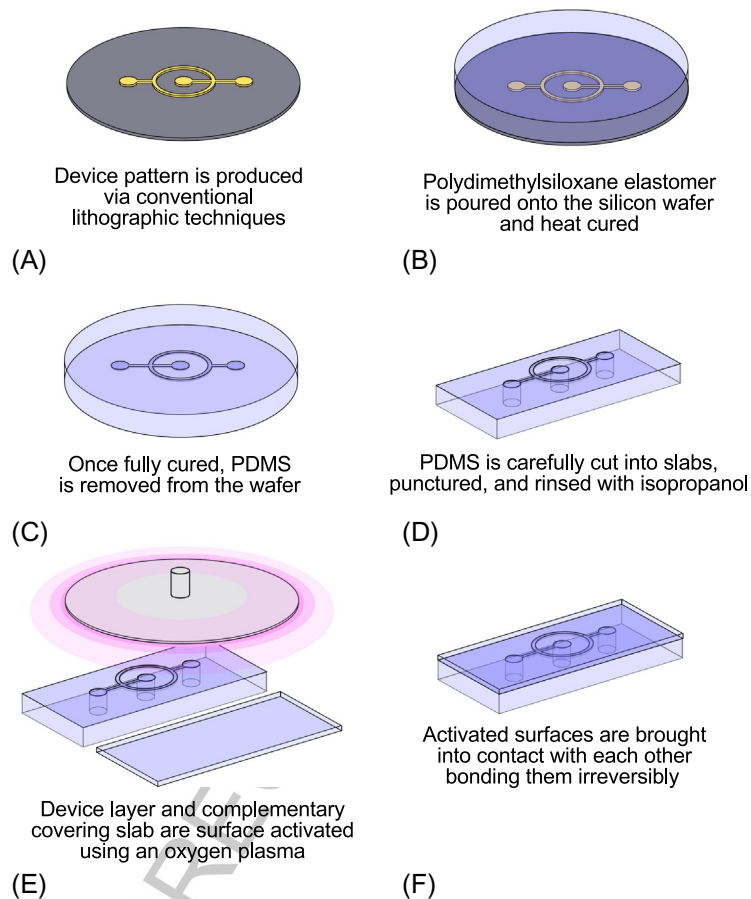
Device pattern is produced
via conventional
lithographic techniques

(A)

Polydimethylsiloxane elastomer
is poured onto the silicon wafer
and heat cured

(B)

Once fully cured, PDMS
is removed from the wafer

(C)

PDMS is carefully cut into slabs,
punctured, and rinsed with isopropanol

(D)

Device layer and complementary
covering slab are surface activated
using an oxygen plasma

(E)

Activated surfaces are brought
into contact with each other
bonding them irreversibly

(F)

Fig. 5

f0030 Assembly of a polydimethylsiloxane microfluidic device. (A) a design wafer is produced. (B) PDMS is poured onto the wafer, thoroughly degassed, and heat cured. (C) PDMS is carefully removed from the wafer. (D) PDMS is cut into shape, punctured, and cleaned with isopropanol. (E) PDMS and complementary covering slab is plasma treated to surface activate. (F) Activated surfaces are brought together to allow irreversible bonding. Device is now complete.

s0160 **6.5.3.1 Photolithographic Manufacture**

p0330 Photolithographic manufacture of PDMS microfluidics is a powerful assembly method which involves the manufacture of a negative pattern or mold onto which the PDMS is cast and cured [53]. Conventional photolithographic manufacture proceeds as follows: first a device design is produced and printed on a mask, this can either be a transparency foil, or for higher resolution applications, a patterned chrome layer on a quartz slab. This mask is used as the photoresist exposure mask during lithography.

p0335 Next, a photo resist (usually SU-8, an epoxy-based negative resist, with favorable viscosity allowing suitable maximum feature depth) is applied to a silicon wafer and spin coated to the

desired thickness. This photoresist is then UV treated in a mask aligner, using the device pattern mask to selectively occlude the device features. The exposed photoresist is then treated with a developing agent, leaving behind a positive relief structure of the desired microfluidic pattern. Finally, this pattern can be treated with a lift-off agent in order to reduce the likelihood of PDMS sticking to it.

s0165 ### 6.5.3.2 Plasma Bonding

p0340 When a PDMS surface is exposed to an oxygen plasma, the surface is bombarded by a range of high-energy species including oxygen radicals, ozone, and oxygen ions. The impacts of these species with the PDMS surface replaces the surface methyl groups of the PDMS with silanol groups, activating the surface of the elastomer. When this activated surface is brought into contact with silanol groups on a complementary bonding surface, either glass or PDMS, the surface silanol groups undergo a condensation reaction irreversibly binding the surfaces together. This process is shown schematically in Fig. 6.
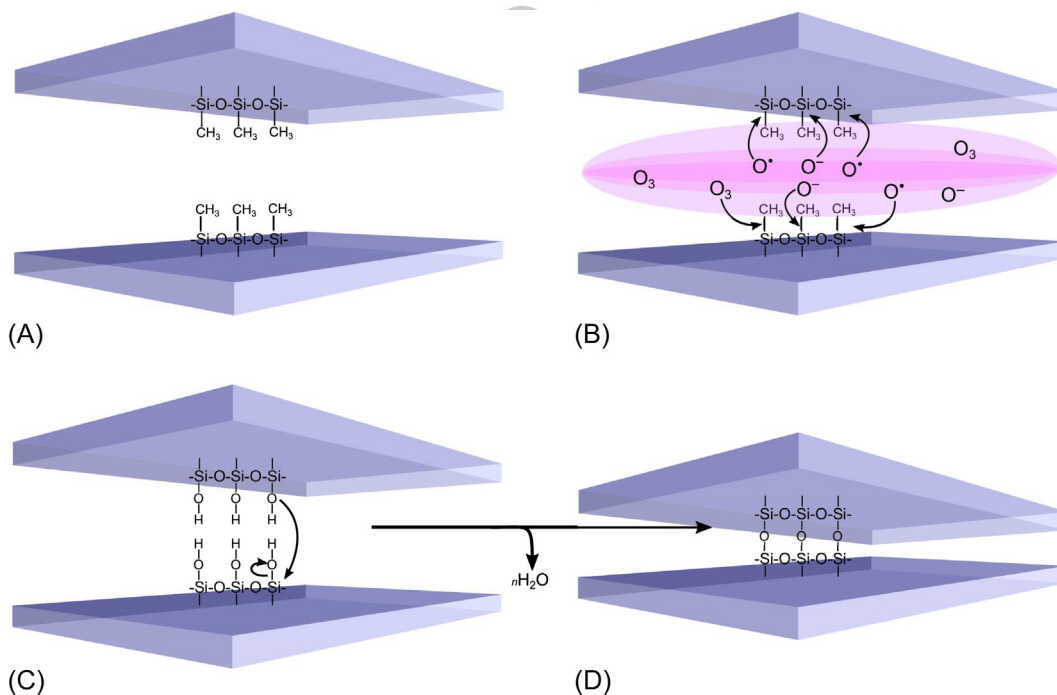
Fig. 6

f0035 Mechanism of plasma bonding PDMS surfaces. (A) Natively PDMS surfaces have a high prevalence of methyl groups, these methyl groups can be converted into silanol groups via plasma activation. (B) In plasma activation highly energetic species such as ozone, oxygen radicals, and oxygen ions attack the surface methyl groups replacing them with silanol groups. (C) When brought into close proximity with a complementary surface, the silanol groups undergo a condensation releasing water. (D) Finally, the condensation of the two surfaces yields an irreversible molecular bond between the two PDMS surfaces.

6.5.4 Surface Properties

p0345 Due to the silicone moieties located on the bulk polymer surface, native PDMS is a tremendously hydrophobic polymer. This makes PDMS devices most suitable for either entirely oil phase systems, or multiphase water-in-oil systems. However, when working with any primarily aqueous phases, this surface hydrophobicity interferes with and disrupts the fluid flow. Additionally, even in an optimal fluid system, this hydrophobic surface can be rapidly contaminated by other hydrophobic components in the flow, fouling the channels.

p0350 While PDMS is clearly a powerful material for microfluidic systems, this hydrophobicity presents a challenge for the wider adoption of PDMS. In order to allow PDMS to be successfully used with aqueous systems, one must modify the surface properties. This can be carried out in a range of methods including gas-phase treatments, liquid-phase treatments, and combinations of the two. These procedures are of primary relevance for oil-in-water emulsions. The hydrophobic surfaces of PDMS inhibit the formation of a stable oil-in-water interface, interfering with the mechanism of droplet generation.

s0175 ### 6.5.5 Gas-phase Processing

s0180 #### 6.5.5.1 Plasma Treatment

p0355 As discussed in Section 6.5.3.2, plasma treatment of PDMS involves exposure of the surface to a plasma, usually oxygen. This plasma can be generated via corona discharges, radio frequencies, or gas arcs, and in addition to facilitating PDMS bonding has a large impact on the surface properties of a microfluidic device [54].

p0360 Plasma modification employs gases such as oxygen, nitrogen, or hydrogen to modify the substrate surface. Of these oxygen plasma treatment is by far the most common surface modification method employed in microfluidics [55–58].

p0365 The exact reactions that occur on the PDMS surface are highly complex, and consequently the mechanisms involved are poorly understood. When the plasma is applied to the surface, the surface is simultaneously subjected to a range of high-energy species including electrons, ozone, ions, and radiation.

p0370 What is known about the overall effects of the plasma exposure is that two main processes dominate this process: (i) there is the formation of silanol groups at the surface, these then condense into a SiO_x silica like layer with a higher oxygen content than the bulk PDMS, and (ii) the replacement of this silica layer with low molecular weight PDMS groups.

p0375 X-ray photoelectron spectroscopy (XPS) carried out by various groups[59–64] shows that as PDMS exposed to a plasma is oxidized, there is a clear increase in oxygen content and a decrease in carbon content. Resolution of the XPS peaks showed that the condensation of the

silanols leads to the formation of a Si-O-Si structure. However, focusing on surface chemistry does not provide a complete picture with regard to hydrophilicity. Plasma treatment, in addition to chemically modifying the surface of PDMS also significantly affects the nanoscopic structure of the surface. This surface roughening is thought to contribute to PDMS becoming hydrophilic after plasma treatment.

p0380 Regardless of the mechanism involved, however, plasma oxidation remains an extremely powerful tool to produce a hydrophilic surface with experiments showing reductions in water contact angle of up to 80° [65]. However, while significantly more hydrophilic than native PDMS, this plasma oxidized surface is not particularly stable, and rapidly undergoes hydrophobic recovery.

p0385 Once again, the mechanism by which this recovery occurs is unclear, but is assumed to be one of the following processes: (i) reorientation of the surface silanol groups into the bulk polymer, (ii) cracking of the SiO_x structure, providing voids within which free PDMS chains can migrate to the surface, (iii) condensation of the silanol groups at the surface, (iv) loss of volatile oxygen rich species, and (v) changes in the surface roughness. Of these, it is widely accepted that the migration of free PDMS chains to the surface is the dominant mechanism [66].

s0185 ### 6.5.5.2 UV Treatment

p0390 Almost an order of magnitude slower than plasma treatment, UV treatment can nevertheless achieve similar reductions in water contact angle on a PDMS surface [67]. One advantage of this technique, however, is that due to the optical transparency of PDMS, UV modification can reach much deeper into the bulk material. This of course reduces the rate of hydrophobic recovery.

s0190 ### 6.5.5.3 Chemical Vapor Deposition

p0395 Chemical vapor deposition or CVD is a process which can be used to produce a thin film of a substance on a substrate surface by depositing gaseous molecules of the film substance onto the substrate surface [54, 55]. Typically CVD proceeds via sublimation of the film substance, pyrolysis, and deposition. This technique has been used in the past to deposit polymers on the inside surfaces of preassembled PDMS devices, however, this technique still has some limitations in terms of film uniformity[68].

s0195 ### 6.5.5.4 Polymer Electrolyte Coating

p0400 In this method, first the PDMS chip is fully assembled using the conventional plasma treatment method. Once is done polymer solutions are flown through the sample at predetermined flow rates. This is done in sequential "plugs" of two different polymers. This allows sequential buildup of both a binding polymer and the hydrophilic polymer that will be used as the primary surface coating.

s0200 *6.5.5.5 Layer-by-Layer Deposition*

p0405 One rapidly emerging modification method is the layer-by-layer assembly technique. Layer-by-layer deposition involves the alternating adsorption of polyanions and polycations to produce a polymer electrolyte multilayer (PEM). One advantage of this method is that this polymer adsorption can occur on virtually any substrate [69].

p0410 Layer-by-layer PEM surface coatings have many advantages over gas-phase treatments including simplicity, efficiency, and excellent control over layer thickness. However, the PEM structure and stability are highly dependent on a range of parameters including polyelectrolyte ionic strength and concentration, solvent composition, and temperature and pH of the solution [70].

s0205 *6.5.5.6 Sol-Gel Processing*

p0415 Sol-gel processing refers to a coating process based on the transition between a liquid solution containing suspended particles to a solid-like gel state. As these coatings provide a high density and homogeneous distribution of cross-linked particles, sol-gel coatings are advantageous for PDMS surface modification [55, 71].

s0210 *6.5.5.7 Surface Activated Liquid-Phase Treatments*

p0420 The treatments described above require no pretreatment of the PDMS, allowing them to be used without access to a sophisticated fabrication laboratory. However, the combination of surface activation treatments such as plasma activation or UV irradiation with polymer deposition allows for the formation of extremely robust device surfaces. These surface activated deposition treatments function via chemical bonding of the polymer in suspension to the PDMS surface.

p0425 One example of a surface activated liquid-phase treatment is the aforementioned layer-by-layer deposition on a plasma activated PDMS device. This technique was demonstrated by Bauer et al. who used alternating treatments of poly(sodium 4-styrenesulfonate) and poly allylamine hydrochloride. One particular strength of their method was the application of the polymer via microfluidic methods. By using syringe pumps and tubing to deliver the polymer solutions, it is possible to selectively coat only the regions of interest within the channel. This method allowed Bauer et al. to selectively hydrophilicize droplet generation geometries to allow the generation of water-in-oil in water double emulsions [72].

p0430 An alternative method which achieves similar results without requiring time consuming layer-by-layer application process is the deposition of polyvinyl alcohol (PVA) into plasma activated microfluidic channels [73]. Plasma activation of the PDMS surfaces introduces hydroxyl moieties onto the elastomer surface, allowing hydrogen-bonding between the PVA and the PDMS surface [74]. By exploiting the hydrophobic interactions between the alkyl

groups and the hydrogen bonding between the hydroxyl groups, this treatment can be used to assemble multilayer PVA coatings via a single liquid treatment [75].

p0435   Finally, a very versatile treatment is surface silanization. Surface silanization can be performed on most substrates which contain surface hydroxyl groups [55], and thus can be utilized with any surface activated PDMS substrate. These hydroxyl groups react with alkoxysilanes to form covalent Si-O-Si bonds to the underlying substrate. Amine, thiols, or carboxyl terminated alkoxysilanes allow the introduction of various functional headgroups onto the surface [76].

s0215   ## 6.6 *Norland Microfluidics*

p0440   Producing suitable oil-in-water emulsions via microfluidic methods remains challenging. As discussed in Section 6.5.4 the vast majority of microfluidic emulsification systems are manufactured using PDMS. While PDMS is an excellent material for water-in-oil microfluidics [77] offering good solvent compatibility, good optical transmissivity, high flexibility, and great durability, it is also strongly hydrophobic, preventing the stable formation of oil-in-water droplets [54]. Although techniques for making PDMS devices hydrophilic, thereby allowing stable droplet generation exist, these are either short lived such as plasma treatment [66] or involve sequential surface coatings [72] which are impractical for use with devices small enough to easily generate micron-scale droplets. Additionally, PDMS is highly porous, leading to high degree of swelling when exposed to many commonly found oils and solvents [78]. By warping and deforming the sensitive droplet generation geometries, this swelling significantly narrows the range of liquids which can be used in PDMS devices.

p0445   Norland optical adhesives provide a viable alternative to PDMS for oil-in-water microfluidics [79, 80] allowing rapid templating of complex microchannels [81]. Their rapid curing speed, alongside their durability, makes them ideal for pattern transfer from PDMS molds. Additionally, while natively more hydrophilic than PDMS, exposure to an oxygen plasma forms a long-lasting hydrophilic surface, ideal for the formation of oil-in-water droplets [79].

p0450   As a family of rapid-UV curing adhesives designed for optics applications, Norland optical adhesives are available in a large range of formulations. These formulations each consist of a proprietary blend of UV curing photo polymers, and have notably different curing rates, optical transparencies, and mechanical properties. For microfluidic purposes, the most suitable product is NOA 81. This formulation cures very rapidly, fully curing under long-wave UV radiation in mere minutes and thus is most suitable for the in situ curing required for the manufacture of microfluidic devices. In order to quantify how NOA-based devices improve upon the surface properties of PDMS, contact angle experiments were carried out. All contact angle measurements were carried out on a Krüss DS4 sessile drop tensiometer. Water contact angle measurements were carried out for both PDMS and NOA 81, both before and immediately after plasma treatment.
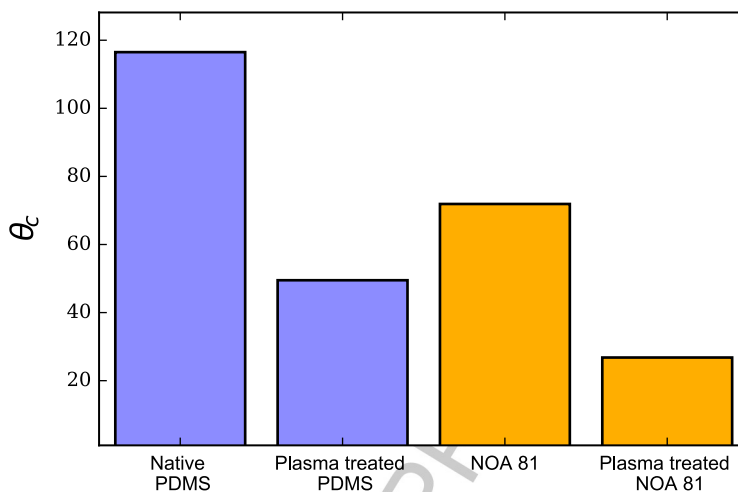
Fig. 7

f0040   Water contact angle measurements PDMS and NOA 81, both before and after treatment with an oxygen plasma.

p0455   The results shown in Fig. 7 indicate that plasma treatment of NOA 81 leads to a reduction in water contact angle of approximately 80 degrees. However, as NOA adhesives are UV cured, they are far more rigidly cross-linked, and the hydrophilic surface does not deteriorate over time as in the case of PDMS. Due to this, plasma treated NOA 81 surfaces remain hydrophilic for several weeks or months.

6.7 Droplet Microfluidics

p0460   The controllable production of micron-scale emulsions, often referred to as microdroplets or nanoemulsions, is an area of highly active research due to their countless technological and research applications. One method which offers a promising route to the controllable production of microdroplets is microfluidics. While applications of microfluidic systems can be found across a wide range of research topics, microfluidic emulsification has proven itself in particular as a powerful tool for both medical diagnostics and synthetic biology [33]. In these fields the applications of microfluidics include the generation of artificial cells [82] and high-throughput screening of patient samples [83–85]. However, despite their many applications, the production of droplets below 10 μm in diameter via microfluidic means provides a significant challenge (Table 2).

p0465   Droplet production in any microfluidic droplet generator proceeds via much the same general scheme: two or more immiscible fluids are brought together in a microfluidic channel, leading to the formation of an interface. This interface is then destabilized, breaking up into droplets. This destabilization can occur either via active means such as the application of a field, whether electric, ultrasonic, or otherwise, or via passive means where the break up is induced purely via geometric means.

t0015 **Table 2: Comparison of microfluidic droplet generation methods.**

| Droplet Generation Method	Emulsion Type	Water Droplet Diameter	Oil Droplet Diameter
T-junction droplet generation	Water-in-oil [86] or oil-in-water [87]	50 μm	100 μm
Capillary coflow droplet generation	Water-in-oil or oil-in-water [88]	20 μm	10 μm
Flow focusing	Water-in-oil [89] or oil-in-water [90, 91]	10 μm	20 μm
Partial wetting	Fluorinated oil-in-water [92]	—	6 μm
Geometric breakup	Water-in-oil [93]	50 μm	—
Tip-streaming	Water-in-oil [94]	3 μm	—
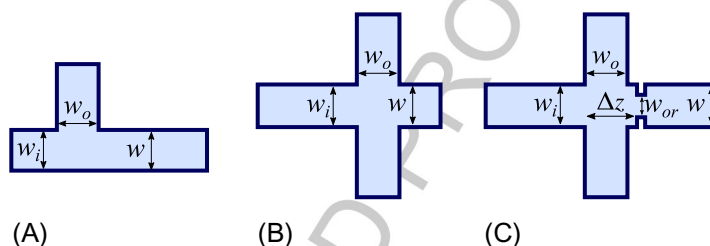
Fig. 8

f0045 Common droplet microfluidics geometries: (A) T-junction device. (B) Coflow device, and (C) Flow focusing device.

s0225 ### 6.7.1 Passive Droplet Microfluidics

p0470 In a general case, droplet breakup of a fluid is primarily driven by the Rayleigh–Plateau instability. This instability, named after Joseph Plateau and Lord Rayleigh in the late 1800s, was originally described by Plateau in terms of a stream of water dropped from a fixed height. This instability arises from the interplay between minute instabilities in the fluid; these instabilities or perturbations, omnipresent regardless of the stability of the flow, can be broken up into those which grow smaller with time and those which grow larger. By mapping these perturbations into sinusoidal components along the direction of fluid flow, Rayleigh demonstrated mathematically that a circular column of nonviscous fluid dropped from height would break up into droplets if the wavelength of the perturbations is larger than the circumference of the stream [95]. It is important, however, to note that due to the confinement in microfluidic system, this instability can often be delayed, or even suppressed. This modification of the device geometry to directly influence the droplet breakup of a fluid flow, and is the fundamental principle governing passive droplet generation.

p0475 In a passive microfluidic device, generally, microfluidic droplet generation is achieved via three main geometries as shown in Fig. 8: (A) T-junctions in which viscous shear stress at one fluid interface pull off droplets into the flow of second immiscible fluid [96], (B) coflowing devices in which a continuous phase fluid flows parallel to and surrounding a second fluid. The interface between these fluids then stretches along the direction of flow, until ultimately it

snaps and droplet generation occurs [97], and flow-focusing devices, where coflowing fluids are forced through a flow constriction, leading to the formation of a velocity gradient along the fluid tendril, and thus droplet breakup [89].

p0480 While they offer some insight into the behavior of a system, analytical solutions to the microfluidic flows are not generally possible due to the complexity involved in the geometry of microfluidic channels and the deformable interface between the fluids of interest. Instead, numerical simulations focus on the controlling dimensionless parameters described earlier.

p0485 In addition to the general dimensionless parameters described earlier microfluidic flow in a two-phase system is governed by several primary parameters including, the capillary number described earlier, here expressed in a form specific to microfluidic devices $Ca = \mu_o U/\gamma = \mu_o G a_0/\gamma$, the flow rate ratio between the droplet and the continuous fluid, $R = Q_i/Q_o$, and the viscosity ratio of the two fluids $\lambda = \mu_i/\mu_o$. The dimensional variables that make up these crucial dimensionless parameters are the volumetric flow rate Q, the viscosity η, and the interfacial tension λ, with the subscripts i and o referring to the inner and outer fluid, respectively. These parameters are constant across all forms of microfluidic geometries, but the characteristic velocity U is defined differently for each of the different microfluidic devices. For example, the capillary number in cross-flow geometries is typically defined in terms of a the mean velocity of the outer fluid $U = Q_o/wh$, where w and h are the width and depth of the downstream channel, respectively [98, 99], whereas for flow-focusing geometries the capillary numbers is defined in terms of the axial elongation rate in the flow focusing aperture,

$$G = \frac{Q_o}{h \Delta z} \left(\frac{1}{w_{or}} - \frac{1}{2w_o} \right) \tag{10}$$

p0490 where Δz is the axial distance between the end of the inlet channel for the dispersed phase and the flow-focusing orifice of width w_{or}. The width w_o is that of the inlet channel for the continuous phase [100]. The characteristic droplet radius is given by half the width of the dispersed phase channel, $a_o = w_i/2$ [98].

p0495 While microfluidic geometries can vary considerably in their design, the mechanisms for droplet and bubble formation are similar across most geometries. These mechanisms can be broadly divided into three regimes: squeezing, dripping, and jetting. While substantially different from each other, one factor that must be consistent across all modes of droplet generations is the assumption of uniform surface tension across the interface between the droplet and the continuous fluid. This surface tension uniformity can be experimentally achieved via either a system without any surfactant or a system with sufficient surfactant such that interfacial tension can be taken as the bulk concentration equilibrium. Given one can obtain a system in which the surface tension is uniform, the first of these regime one is likely to encounter is the squeezing mode of droplet formation.

s0230 *6.7.1.1 Squeezing*

p0500   When the capillary number is below $Ca < 0.01$, viscous stresses acting on the droplet flow are not sufficiently large to overcome the confining effects of the microchannel walls, and the channel geometry strongly affects the droplet formation. In these devices, the emerging fluid interface grows in size until it fully obstructs the contraction region. Once this region of the channel is fully obstructed, the interface narrows until a droplet breaks off. In order to observe the exact breakup mechanism, Abate et al. used Laplace pressure sensors built into the geometry of a device to observe the local pressures both upstream and downstream during droplet generation.

p0505   In flow-focusing geometries and T-junction devices it was observed that the pressure in the continuous phase liquid upstream rises sharply as the droplet obstructs the downstream channel. As the fluid neck thins and pinches off, the pressure in the fluid eventually reaches a maximum and then decreases. The pressure of the dispersed phase decreases and increases out of phase with the pressure variation of the continuous phase. The downstream pressure on the other hand remains relatively constant [98].

p0510   The large pressure differential between the upstream and downstream areas of the channel forces the interface toward the break off location, causing it to narrow proportionally to the velocity of the liquid. Thus droplet size can be expected to be linearly proportional to both the ratio of the flow rates and the channel width. The exact nature of the breakup mechanism in squeezing microfluidics has long been debated. While early arguments focused on the classic capillary breakup mechanism [101], strong confinement was found to completely suppress capillary instabilities [102]. Additionally, experimental imaging of the interface during breakup shows that unlike conventional droplet breakup, in a confined system the interface narrows in quasi-static manner until final stages of droplet breakup where thread thinning and fluid thread collapse occur [98, 103].

s0235 *6.7.1.2 Dripping and Jetting of Fluid Threads*

p0515   At larger capillary numbers, on the order of $Ca > 0.1$, the fluid interface is more robust, and does not break as readily. This causes coflowing fluid threads to form, regardless of the microfluidic geometry. Here the fluid thread diameter d_t scales with the flow rate ratio. Breakup of this fluid thread is delayed compared to the standard stability theory for viscous and inviscid jets, this delay is largely dependent on the degree of confinement in the device. At extremely high degrees of confinement, where the jet radius is larger than the depth of the channel, the instability is entirely suppressed and the fluid does not form droplets. Less confined fluid threads are always unstable [102], but thread breakup is delayed due to the presence of nearby walls [104, 105].

p0520   In the presence of fluid flow, confined fluids can produce droplets either via the dripping or jetting mechanism [106]. Dripping is characterized by a narrowing thread, and results in

highly uniform droplets. The droplet formation occurs via a fluid thread which undergoes an absolute instability with a stationary breakup location. Jetting on the other hand, which is characterized by a widening thread leads to less uniform droplets, where the breakup occurs via a convective instability that moves along the length of the thread [107]. The exact point at which a fluid thread transitions from a dripping regime to a jetting regime largely depends on both the capillary number of the outer flow, and the Weber number of the inner flow. When viscosity and capillary forces are dominant a narrowing thread occurs, while a widening thread occurs when inertial and capillary forces dominate.

p0525 In the narrowing regime in particular, viscous stress can be so significant that fluid threads form with extremely narrow dimensions, producing droplets with diameters up to 100-fold narrower than the inner fluid thread radius. These narrow threads commonly occur in the absence of inertia, with Reynolds numbers, $Re \ll 1$ in conditions where the outer viscous stresses dominate, usually in systems with viscosity ratios $\phi \ll 1$. The formation of these extremely narrow threads coincides with the creation of a strong radial inward velocity gradient just downstream of where the dispersed phase fluid emerges into the continuous phase. This generates a velocity gradient along the fluid axis, and the resulting extensional stresses act to both focus and stretch the thread. This suppresses the droplet breakup instability until the velocity gradient diminishes downstream, allowing droplet formation to take place [98].

p0530 Overall, while sharing similarities with conventional droplet breakup mechanisms, the key factor in microfluidic droplet generation is confinement. The extreme degree of confinement found on microfluidic length scales modifies the droplet breakup to such an extent that it is possible to access three distinct breakup mechanisms simply by varying basic flow conditions, allowing careful fine-tuning of both droplet size and droplet size distribution [98].

s0240 ### 6.7.2 Active Droplet Generation

p0535 Active droplet generation microfluidics, while involving unique technical challenges relating the incorporation of electromechanical systems with usually soft microfluidic chips, are nonetheless a powerful class of droplet generator. Exploiting an external stimulus to destabilize the droplet interface rather than geometric means, these methods often offer significantly higher throughput or degrees of control than passive, geometric droplet generators.

p0540 Electric energy can be used to manipulate and enhance droplet generation. In particular direct current electrical fields can lead to significant reductions in droplet volume. This reduction in volume occurs via charge accumulation. When the electric charge is applied, free charges in the water migrate until they hit the oil–water interface where charge accumulates. This charge accumulation induces an electrostatic instability, and serves to accelerate droplet breakup leading to smaller droplets [108].

p0545 A similar method of droplet control is thermal control. This can be done via two different approaches. The first utilizes heating to improve droplet generation by applying resistive heating to the droplet formation junction directly. The second approach uses a focused laser beam in order to achieve localized heating. As viscous and interfacial properties of fluids depend strongly on the temperature of a system, the application of a thermal field can induce significant changes in the capillary number of the fluid flow. As described in earlier sections, the diameter of microfluidic droplets depends heavily on the capillary number, and thus this thermal control can be used to gain fine-grained control over the droplet size [109]. More extreme localized heating such as that induced by a focused pulse laser can induce cavitation. The high intensity of the laser causes localized heating and boiling and rapidly creates a bubble. This phenomenon has been used by Park et al. to produce highly uniform micron-scale droplets, by inducing a pressure spike through cavitation which injects a droplet from the interface into the surrounding continuous phase as shown in Fig. 9 [110].
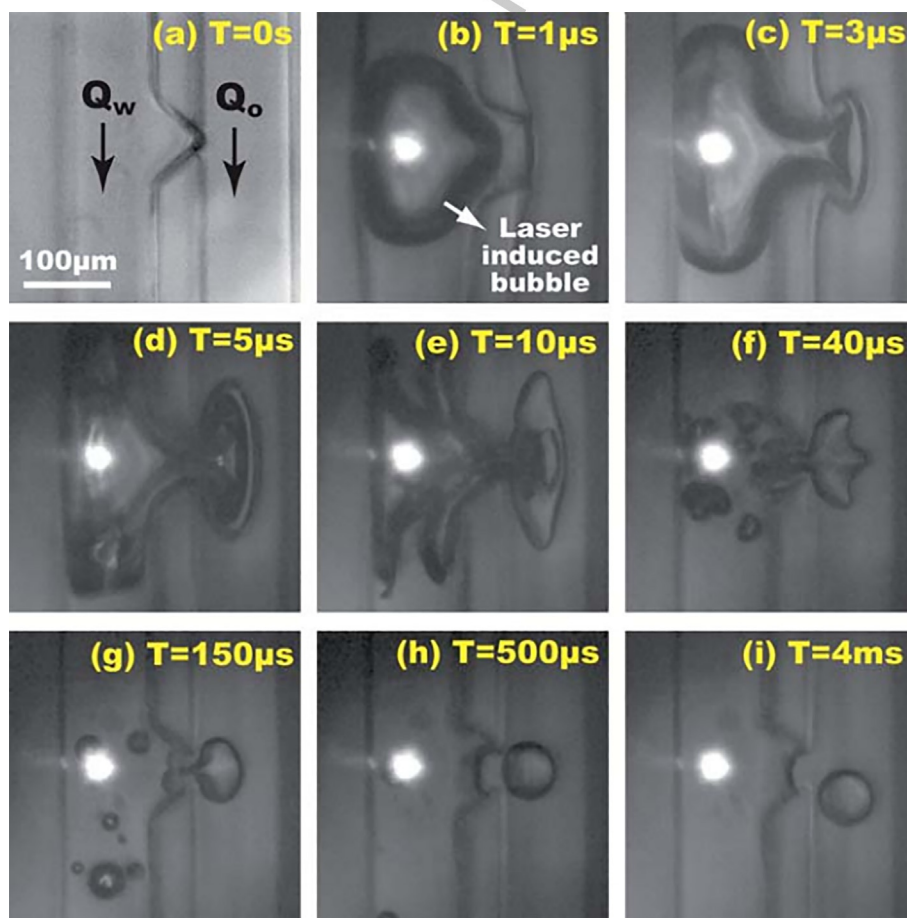

Fig. 9

f0050   Time lapse showing sequence of laser cavitation to produce a microdroplet [110].

p0550 A further method of active droplet generation is mechanical control. In these systems the fluid interface is mechanically deformed via hydraulic, pneumatic, or piezoelectric actuation. Hydraulic and pneumatic actuation is usually executed by valves integrated into microfluidic devices. Generally these valves are made out of the same bulk material as the bulk chip and are operated via compressed air or liquid flowing on a separate control layer. This manipulation of the interface can occur via perturbation of the interface destabilizing it, directly chopping a fluid tendril into droplets, or by varying the droplet geometry in situ. As these methods all rely on direct mechanical modifications of the fluid conditions, these methods tend to be quite slow and imprecise. Piezoelectric actuation on the other hand offers significantly faster response time. Much like pneumatic actuation, piezoelectric actuation can be used to directly dispense droplets, oscillate an interface to induce droplet snap-off, or directly disrupt a fluid tendril via generation of standing acoustic waves.

s0245 ### 6.7.3 Applications of Droplet Microfluidics

p0555 Due to the extremely low sample volumes microfluidic droplet systems involve, droplet microfluidics has become a vital tool in any field which requires high accuracy, low cost, and rapid measurement speeds. In particular, droplet microfluidics has found a niche in the life sciences. Medical diagnostic assays are often prohibitively expensive, or require large amounts of sample, significantly complicating rapid diagnostics. An example of this is flow cytometry, the technique of measuring cell properties under flow. While a powerful technique, this does require significant quantities of cells, often several tens of thousands. While of course for some samples this does not present much of a problem, for the detection of rare objects such as virus infected cells or tumorous tissue smaller sample sizes are required. With the extremely low volume of microfluidic droplets, coupled with the tremendous chemical specificity allowed by droplet encapsulation, droplet microfluidics can improve both the detection threshold and the operation speed of medical diagnostic procedures [111].

s0250 #### 6.7.3.1 Droplet Microfluidics in Medical Research

p0560 First utilized in diagnostic systems, medical microfluidics is a field which has rapidly expanded and has been a field of tremendous scientific impact, with several thousand publications each year. Of these publications, the vast majority are in the field of lab-on-a-chip applications. The applications of medical microfluidics falls broadly into two categories: diagnostic devices and biosensors, with early applications involving the miniaturization of DNA screening. Since these early applications the field has matured somewhat, and today medical microfluidics find application across a broad spectrum.

p0565 In particular, common microfluidic applications seek to overcome technical challenges present in traditional medical assays such as drug screening, disease diagnostics, and cancer screening. The advantage of using microfluidic systems for these challenges is manifold, but primarily lies with the vastly reduced sample volume required. This reduction in sample

volume of course allows the preservation of valuable reagents, allowing significant reduction in cost, or patient trauma by reducing biopsy requirements. Further interest in microfluidic applications arises from the potential for miniaturized point of care (POC) applications where microfluidic systems are directly integrated with sensing modules or sample pretreatments, increasing the efficiency of assays, reducing the risk of cross-contamination, and allowing in situ diagnostics in regions where it may otherwise be impossible. In particular the potential of these devices to carry out complex diagnostic operations without requiring a skilled operator could have a tremendous positive effect on the availability of health-care services in impoverished regions.

p0570 Allowing the analysis of far smaller sample volumes at greater speed, and with significantly higher composition control, research on microfluidic analysis methods for medical applications have long focused on the development of the so-called Micrototal analysis systems (MicroTAS). These devices would allow a whole suite of medical diagnostic tests to be carried out on a single chip, and hold great potential for the future of personalized medicine. A particularly desirable goal is in MicroTAS systems for point-of-care diagnostics (devices where a diagnostic test can rapidly be performed near the patient without the need for a clinical lab). The earliest examples of these applications were applied to the detection of glucose levels, with subsequent development paving the way for self-contained lateral flow tests which require only the addition of a sample. In recent years POC devices have been developed that include disposable microfluidic components allowing low-cost rapid diagnostic testing [28].

p0575 Microfluidic biosensors, on the other hand, offer powerful alternatives to the costly and time-consuming identification methods currently available. This is of particular interest in the field of pathogen sensing where low sample volumes and critical time constraints provide a distinct demand for rapid diagnosis and sensing. MicroTAS systems here offer distinct improvements in terms of analytical performance and sample analysis speed. In addition to their applications in biosensing, utilizing droplet microfluidics for clinical applications allows complex sample handling and manipulation. Two examples of this are microfluidic polymerase chain reaction (PCR) and sample enrichment via droplet sorting.

p0580 The PCR is a common biochemical technique used in molecular biology to amplify low numbers of DNA segments across several orders of magnitude, generating thousands to millions of copies of the starting DNA segments. PCR is a crucial component of many modern diagnostic tests where vanishingly small samples of pathogen must first be enriched before a diagnosis can be confirmed. Unfortunately, requiring many repeated heating and cooling cycles, PCR is a slow process, with enrichment taking between hours and days. Droplet microfluidics have provided an elegant solution to this issue. Due to the low mass of microdroplets, it is possible to achieve the required heating and cooling cycles simply by passing the droplets through heated channels and allowing them to cool. This method demonstrated by Schaerli et al. in a radial PCR device as shown in Fig. 10 was able to
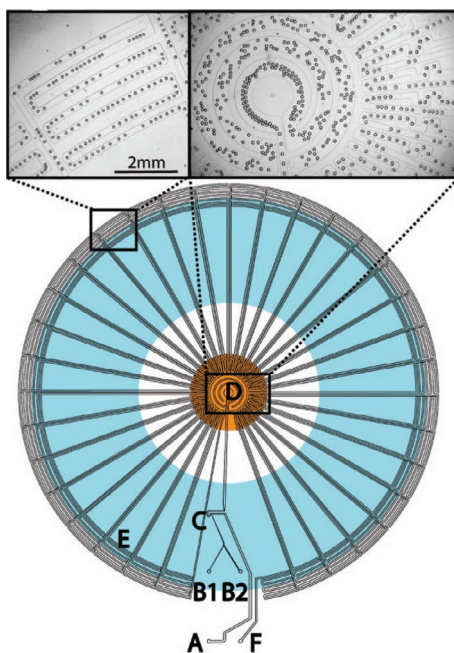
Fig. 10

f0055 Microdroplet PCR. Inlets are marked as B1 and B2, forming droplets at a T-junction (C). The droplets pass into the hot zone of the device (D), the droplets are then annealed (E) and flow back to the center, where the DNA is denatured and the cycle begins, finally the droplets exit the device after 34 cycles. *Adapted with permission from Y. Schaerli, R.C. Wootton, T. Robinson, V. Stein, C. Dunsby, M.A.A. Neil, P.M.W. French, A.J. DeMello, C. Abell, F. Hollfelder, Continuousflow polymerase chain reaction of single-copy DNA in microfluidic microdroplets, Anal. Chem. 81 (1) (2008) 302–306. Copyright 2009 American Chemical Society.*

complete 34 cycles of PCR in just 17 min, reaching amplification factors of up to six orders of magnitude for an 85 base-pair sequence. A feat which would take approximately 2 h via conventional PCR [112].

p0585 Flow cytometry is a technique in which particles, often living cells, are analyzed in flow. This method, commonly functioning by activating a fluorescence signal in target particles, is a crucial to modern clinical research. By allowing the rapid screening and counting of extremely large volumes of particles, cytometry techniques allow for much faster analysis of biological samples. In addition to the applications as an analytical tool, cytometry also allows cell sorting. The most common method, FACS or fluorescence activated cell sorting, sorts cells via the application of a strong electric field which is triggered when the cell of interest is found. However, the fact that the cells being studied must be in a bulk flow for cytometric techniques limits this to systems which do not require compartmentalization of samples. Thus, restricting

the choice of fluorescent markers to ones which remain inside or on the surface of the target cells, making it impossible to study systems with high degrees of enzymatic diffusivity.

p0590   In addition to this limitation, conventional FACS machines require large sample sizes and aerosolize the sample, a significant biosafety concern when working with virulent samples. Microfluidic droplets, however, can be utilized to significantly improve on this technique. Demonstrated by Baret et al. a microfluidic device can be constructed in which target cells are localized and confined in microdroplets. Much like conventional cytometry, these droplets are then passed over a screening laser and if the target signal is detected a field is activated shunting the droplet into the appropriate collection channel. This microfluidic droplet sorter can sort up to 2000 droplets s^{-1}, with unprecedented levels of sorting selectivity. Crucially, unlike FACS, this method allows compartmentalization of samples allowing diffusive enzymes and migrating fluorescent markers to be used (Fig. 11).

s0255   *6.7.3.2 Droplet Microfluidics in Soft Matter Research*

p0595   While the applications of droplet microfluidics in biological or medical fields focus primarily on analysis methods, microfluidics also offers many powerful applications in the field of soft matter. Soft condensed matter as a field shares many similarities with biological applications; the systems are often aqueous, are on comparable length scales, and often benefit equally from miniaturization. In particular the benefits of miniaturization in soft matter are
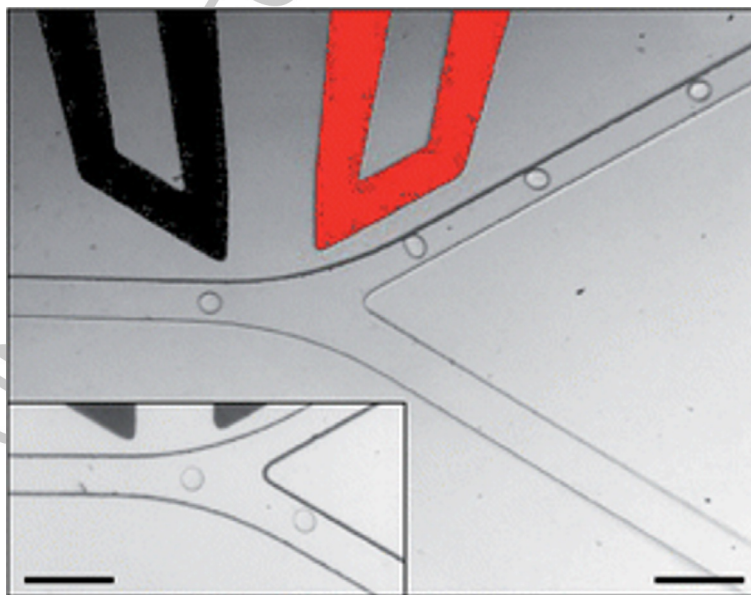

Fig. 11

f0060   Droplet sorting device showing collection and waste channel as well as dielectrophoresis electrode which applies the sorting field [113]. Scale bar represents 100 μm.

twofold, firstly smaller sample sizes allow much faster testing and analysis speeding up experiments, secondly, microfluidic length scales allows probing of the response of soft materials to strong stimulus without requiring high magnitudes of driving fields. This allows strong electric fields, high shear stresses, and large temperature and concentration gradients to be established with very low voltages, fluid velocities and small temperature and concentration gradients, respectively [23].

p0600 With the miniaturization offered by simple microfluidic channels, these find great use to study areas of interest such as droplet deformation [114], diffusive transport of colloidal particles [115], or micro-rheology of soft colloidal suspensions [116]. Droplet microfluidics in particular enable access to a wide range of synthetic methods including the synthesis of hydrogel particles [117], Janus particles [118], complex multilayer emulsions [88], or colloidal molecules [119].

s0260 *6.7.3.3 Droplet Microfluidics for Colloidal Model Systems*

p0605 Earlier in this chapter we discussed colloidal model systems and their use as a powerful research tool across all manner of scientific research. In the context of soft-matter colloidal model systems, droplet microfluidics offers an exciting new route to versatile emulsion-based model systems. While these systems are often challenging to realize experimentally due the small sizes required, recent microfluidic tools, in particular NOA-based microfluidics, has made this significantly easier.

p0610 In particular, devices produced from Norland optical adhesives have been used to generate colloidal droplets as shown in Fig. 12 [31]. These droplets were analyzed via structural analysis tools and a comparison with simulation was carried out. Overall this allowed probing of how an emulsion system might differ from a hard sphere system, and demonstrated that microfluidic emulsions can offer insight into a new class of colloidal system.

s0265 ## 6.8 Conclusions

p0615 Our understanding of complex systems can be greatly enhanced by employing colloidal models. These allow us to theoretically or experimentally probe which would otherwise be inaccessible. The bulk of field concerns itself with solid colloidal particles, however, especially in the field of self-assembly, emulsions offer access to an exciting new parameter space. However, the fabrication of colloidal emulsions is nontrivial with conventional means, and thus an alternative method must be employed. As described above, microfluidic methods offer a powerful route to colloidal emulsions, with several key advantages:
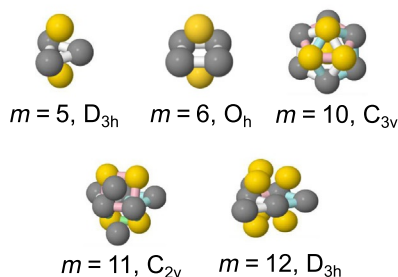
u0010 • Microfluidic devices can be manufactured using a range of manufacturing methods across many different materials, ensuring that these methods are compatible with a wide range of experimental systems.
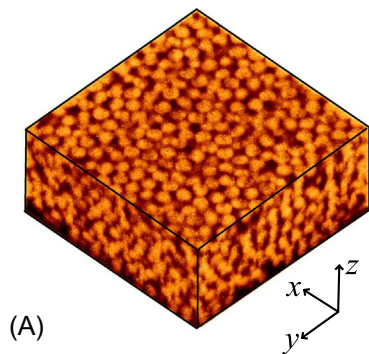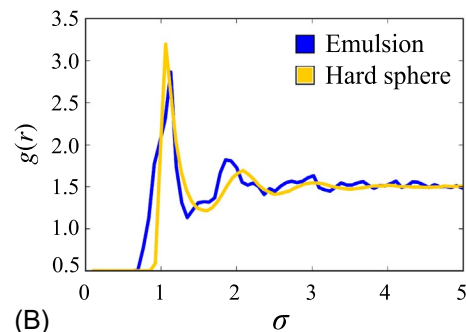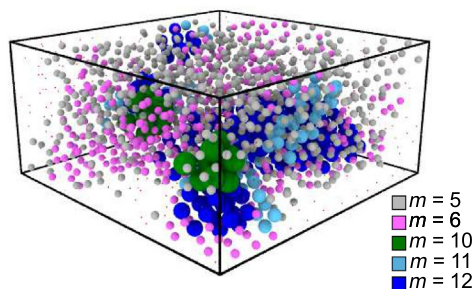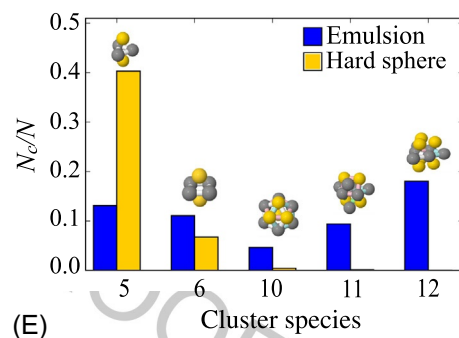
Fig. 12

f0065 Structural analysis of a rather monodisperse colloidal emulsion system. (A) Image showing representation of three-dimensional confocal image of silicone oil emulsion with dimensions of $128.8 \times 128.8 \times 60.1\,\mu m$. (B) Radial distribution function of emulsion droplets in *blue* (*dark gray* in the print version), and a hard sphere system of comparable volume fraction ($\phi = 0.42$) in *yellow* (*light gray* in the print version) with experimental results scaled by the particle diameter. (C) Image showing studied clusters of interest alongside respective point group symmetries. (D) Visualization of cluster distribution on tracked coordinates. (E) Topological cluster classification chart, showing relative population of locally favored icosahedral cluster species for emulsion in blue (*dark gray* in the print version) and hard sphere simulations of comparable volume fraction at relative standard deviations of 8% and 4.8% in *orange* (*gray* in the print version) and *yellow* (*light gray* in the print version), respectively. *Reproduced with permission from M. Meissner, J. Dong, J. Eggers, A.M. Seddon, C.P. Royall, Oil-in-water microfluidics on the colloidal scale: new routes to self-assembly and glassy packings, Soft Matter 13 (2017) 788–794, https://doi.org/10.1039/C6SM02390H, originally published by The Royal Society of Chemistry.*

u0015 • Droplet generation in microfluidic devices commonly proceeds via three main mechanisms: squeezing, dripping, and jetting. These mechanisms can all be accessed in situ allowing for exceptional control over droplet size and conventional emulsification techniques.

u0020 • Microfluidic droplet generators currently find applications primarily in biological research, where they serve as powerful analytical tools for point-of-care diagnostics.

u0025 • However, aside from their analytical applications droplet microfluidics offers an exceptional range of new synthetic techniques. Capable of producing colloidal emulsions, Janus particles, elaborately shaped hydrogels, or as an encapsulation tool, the potential of droplet microfluidics as a synthetic tool seems limitless.

p0640 Overall, in addition to their proven track record for biological applications, microfluidic tools offer exciting new avenues for soft matter research. Enabling both the probing of systems otherwise hard to access, and novel synthetic routes to complex materials it is clear that a thorough understanding of microfluidic systems, and in particular, microfluidic droplet generators is of great use for designing the soft matter experiments of the future.

st0280 ## *References*

[1] A. Adúriz-Bravo, A 'semantic' view of scientific models for science education, Sci. Educ. 22 (7) (2013) 1593–1611.

[2] D.M. Bailer-Jones, Scientists' thoughts on scientific models, Perspect. Sci. 10 (3) (2002) 275–301.

[3] J. Perrin, Atoms, Constable & Company, 1916.

[4] W. Poon, Colloids as big atoms, Science 304 (5672) (2004) 830–831.

[5] T.F. Tadros, Encyclopedia of Emulsion Technology, in: P. Becher (Ed.), vol. 1, Marcel Dekker, New York, 1983.

[6] C.P. Royall, W.C.K. Poon, E.R. Weeks, In search of colloidal hard spheres. Soft Matter 1744-683X9 (1) (2013) 17–27, https://doi.org/10.1039/c2sm26245b.

[7] J. Bibette, T.G. Mason, H. Gang, D.A. Weitz, Kinetically induced ordering in gelation of emulsions, Phys. Rev. Lett. 69 (6) (1992) 981.

[8] J.N. Wilking, S.M. Graves, C.B. Chang, K. Meleson, M.Y. Lin, T.G. Mason, Dense cluster formation during aggregation and gelation of attractive slippery nanoemulsion droplets, Phys. Rev. Lett. 96 (1) (2006) 015501.

[9] L.J. Teece, M.A. Faers, P. Bartlett, Ageing and collapse in gels with long-range attractions, Soft Matter 7 (4) (2011) 1341–1351.

[10] T.M. Obey, B. Vincent, Novel monodisperse "silicone oil"/water emulsions, J. Colloid Interface Sci. 163 (2) (1994) 454–463.

[11] G.M. Whitesides, The origins and the future of microfluidics, Nature 442 (7101) (2006) 368–373.

[12] J.S. Mellors, K. Jorabchi, L.M. Smith, J.M. Ramsey, Integrated microfluidic device for automated single cell analysis using electrophoretic separation and electrospray ionization mass spectrometry, Anal. Chem. 82 (3) (2010) 967–973.

[13] C.B. Rohde, F. Zeng, R. Gonzalez-Rubio, M. Angel, M.F. Yanik, Microfluidic system for on-chip high-throughput whole-animal sorting and screening at subcellular resolution, Proc. Natl. Acad. Sci. 104 (35) (2007) 13891–13895.

[14] E. Brouzes, M. Medkova, N. Savenelli, D. Marran, M. Twardowski, J.B. Hutchison, J.M. Rothberg, D. R. Link, N. Perrimon, M.L. Samuels, Droplet microfluidic technology for single-cell high-throughput screening, Proc. Natl. Acad. Sci. 106 (34) (2009) 14195–14200.

[15] S. Marre, K.F. Jensen, Synthesis of micro and nanostructures in microfluidic systems, Chem. Soc. Rev. 39 (3) (2010) 1183–1202.

[16] H. Song, R.F. Ismagilov, Millisecond kinetics on a microfluidic chip using nanoliters of reagents, J. Am. Chem. Soc. 125 (47) (2003) 14613–14619.

[17] L. Shui, S. Pennathur, S. Pennathur, J.C.T. Eijkel, A. van den Berg, Multiphase flow in lab on chip devices: a real tool for the future? Lab Chip 8 (7) (2008) 1010–1014.

[18] N.J. Nielsen, History of ThinkJet printhead development, Hewlett-Packard J. 36 (5) (1985) 4–10.

[19] R.P. Feynman, There's plenty of room at the bottom, Eng. Sci. 23 (5) (1960) 22–36.

[20] S.C. Terry, J.H. Jerman, J.B. Angell, A gas chromatographic air analyzer fabricated on a silicon wafer, IEEE Trans. Electron Devices 26 (12) (1979) 1880–1886.

[21] D.C. Duffy, J.C. McDonald, O.J.A. Schueller, G.M. Whitesides, Rapid prototyping of microfluidic systems in poly(dimethylsiloxane), Anal. Chem. 70 (23) (1998) 4974–4984.

[22] T. Thorsen, S.J. Maerkl, S.R. Quake, Microfluidic large-scale integration, Science 298 (5593) (2002) 580–584.

[23] D. Bartolo, D.G. Aarts, Microfluidics and soft matter: small is useful, Soft Matter 8 (41) (2012) 10530–10535.

[24] B.H. Weigl, P. Yager, Microfluidic diffusion-based separation and detection, Science 283 (5400) (1990) 346–347.

[25] A.E. Kamholz, B.H. Weigl, B.A. Finlayson, P. Yager, Quantitative analysis of molecular interaction in a microfluidic channel: the T-sensor, Anal. Chem. 0003270071 (23) (1999) 5340–5347, https://doi.org/10.1021/ac990504j.

[26] X. Li, D.R. Ballerini, W. Shen, A perspective on paper-based microfluidics: current status and future trends, Biomicrofluidics 6 (1) (2012) 011301.

[27] E. Carrilho, A.W. Martinez, G.M. Whitesides, Understanding wax printing: a simple micropatterning process for paper-based microfluidics, Anal. Chem. 81 (16) (2009) 7091–7095.

[28] S.K. Sia, L.J. Kricka, Microfluidics and point-of-care testing, Lab Chip 8 (12) (2008) 1982–1983.

[29] J.B. Knight, A. Vishwanath, J.P. Brody, R.H. Austin, Hydrodynamic focusing on a silicon chip: mixing nanoliters in microseconds, Phys. Rev. Lett. 80 (17) (1998) 3863.

[30] C.-W. Tsao, D.L. DeVoe, Bonding of thermoplastic polymer microfluidics, Microfluid. Nanofluid. 6 (1) (2009) 1–16.

[31] M. Meissner, J. Dong, J. Eggers, A.M. Seddon, C.P. Royall, Oil-in-water microfluidics on the colloidal scale: new routes to self-assembly and glassy packings, Soft Matter 13 (2017) 788–794, https://doi.org/10.1039/C6SM02390H.

[32] A.M. Gañán-Calvo, R. González-Prieto, P. Riesco-Chueca, M.A. Herrada, M. Flores-Mosquera, Focusing capillary jets close to the continuum limit, Nat. Phys. 1745-24733 (10) (2007) 737–742, https://doi.org/10.1038/nphys710.

[33] D.J. Beebe, G.a. Mensing, G.M. Walker, Physics and applications of microfluidics in biology, Annu. Rev. Biomed. Eng. 1523-9829, 4 (2002) 261–286, https://doi.org/10.1146/annurev.bioeng.4.112601.125916. http://www.ncbi.nlm.nih.gov/pubmed/12117759.

[34] G.D. Aumiller, E.A. Chandross, W.J. Tomlinson, H.P. Weber, Submicrometer resolution replication of relief patterns for integrated optics, J. Appl. Phys. 45 (10) (1974) 4557–4562.

[35] S. Masuda, M. Washizu, T. Nanba, Novel method of cell fusion in field constriction area in fluid integration circuit, IEEE Trans. Ind. Appl. 25 (4) (1989) 732–737.

[36] G.M. Whitesides, E. Ostuni, S. Takayama, X. Jiang, D.E. Ingber, Soft lithography in biology and biochemistry, Annu. Rev. Biomed. Eng. 3 (1) (2001) 335–373.

[37] L. Martynova, L.E. Locascio, M. Gaitan, G.W. Kramer, R.G. Christensen, W.A. MacCrehan, Fabrication of plastic microfluid channels by imprinting methods, Anal. Chem. 69 (23) (1997) 4783–4789.

[38] J.-W. Choi, S. Kim, R. Trichur, H.J. Cho, A. Puntambekar, R.L. Cole, J.R. Simkins, S. Murugesan, K. Kim, J.-B.J.B.Lee, A plastic micro injection molding technique using replaceable mold-disks for disposable microfluidic systems and biochips, in: Micro Total Analysis Systems 2001, Springer, 2001, pp. 411–412.

[39] C.M.B. Ho, S.H. Ng, K.H.H. Li, Y.-J. Yoon, 3D printed microfluidics for biological applications, Lab Chip 15 (18) (2015) 3627–3637.

[40] A.K. Au, W. Huynh, L.F. Horowitz, A. Folch, 3D-printed microfluidics, Angew. Chem. Int. Ed. 55 (12) (2016) 3862–3881.

[41] D. Gobby, P. Angeli, A. Gavriilidis, Mixing characteristics of T-type microfluidic mixers, J. Micromech. Microeng. 11 (2) (2001) 126.

[42] S.W. Lee, D.S. Kim, S.S. Lee, T.H. Kwon, A split and recombination micromixer fabricated in a PDMS three-dimensional structure, J. Micromech. Microeng. 16 (5) (2006) 1067.

[43] S. Hardt, T. Dietrich, A. Freitag, V. Hessel, H. Löwe, C. Hofmann, A. Oroskar, F. Schönfeld, K.M. Vanden Bussche, Radial and tangential injection of liquid/liquid and gas/liquid streams and focusing thereof in a special cyclone mixer, in: Sixth International Conference on Microreaction Technology, IMRET, vol.6, 2002, pp. 329–344.

[44] S.W. Jones, O.M. Thomas, H. Aref, Chaotic advection by laminar flow in a twisted pipe, J. Fluid Mech. 209 (1989) 335–357.

[45] R.H. Liu, M.A. Stremler, K.V. Sharp, M.G. Olsen, J.G. Santiago, R.J. Adrian, H. Aref, D.J. Beebe, Passive mixing in a three-dimensional serpentine microchannel, J. Microelectromech. Syst. 9 (2) (2000) 190–197.

[46] Z. Yang, S. Matsumoto, H. Goto, M. Matsumoto, R. Maeda, Ultrasonic micromixer for microfluidic systems, Sens. Actuators, A 93 (3) (2001) 266–272.

[47] L.-H. Lu, K.S. Ryu, C. Liu, A novel microstirrer and arrays for microfluidic mixing, in: Micro Total Analysis Systems 2001, Springer, 2001, pp. 28–30.

[48] J.R. Anderson, D.T. Chiu, R.J. Jackman, O. Cherniavskaya, J.C. McDonald, H. Wu, S.H. Whitesides, G. M. Whitesides, Fabrication of topologically complex three-dimensional microfluidic systems in PDMS by rapid prototyping, Anal. Chem. 72 (14) (2000) 3158–3164.

[49] Z. Li, A.M. Leshansky, L.M. Pismen, P. Tabeling, Step-emulsification in a microfluidic device, Lab Chip 15 (4) (2015) 1023–1031.

[50] F. Schuler, F. Schwemmer, M. Trotter, S. Wadle, R. Zengerle, F. von Stetten, N. Paust, Centrifugal step emulsification applied for absolute quantification of nucleic acids by digital droplet RPA, Lab Chip 15 (13) (2015) 2759–2766.

[51] A.E. Vasdekis, M.J. Wilkins, J.W. Grate, R.T. Kelly, A.E. Konopka, S.S. Xantheas, T.M. Chang, Solvent immersion imprint lithography, Lab Chip 14 (12) (2014) 2072–2080.

[52] K.R. Berry Jr., A.G. Russell, P.A. Blake, D.K. Roper, Gold nanoparticles reduced in situ and dispersed in polymer thin films: optical and thermal properties, Nanotechnology 23 (37) (2012) 375703.

[53] Y. Xia, G.M. Whitesides, Soft lithography, Annu. Rev. Mater. Sci. 28 (1) (1998) 153–184.

[54] H. Makamba, J.H. Kim, K. Lim, N. Park, J.H. Hahn, Surface modification of poly(dimethylsiloxane) microchannels, Electrophoresis 01730835, 24 (21) (2003) 3607–3619, https://doi.org/10.1002/elps.200305627.

[55] J. Zhou, A.V. Ellis, N.H. Voelcker, Recent developments in PDMS surface modification for microfluidic devices, Electrophoresis 31 (1) (2010) 2–16.

[56] X. Ren, M. Bachman, C. Sims, G.P. Li, N. Allbritton, Electroosmotic properties of microfluidic channels composed of poly(dimethylsiloxane), J. Chromatogr. B Biomed. Sci. Appl. 762 (2) (2001) 117–125.

[57] J.A. Vickers, M.M. Caulum, C.S. Henry, Generation of hydrophilic poly(dimethylsiloxane) for high-performance microchip electrophoresis, Anal. Chem. 78 (21) (2006) 7446–7452.

[58] S.L. Peterson, A. McDonald, P.L. Gourley, D.Y. Sasaki, Poly(dimethylsiloxane) thin films as biocompatible coatings for microfluidic devices: cell culture and flow studies with glial cells, J. Biomed. Mater. Res. A 72 (1) (2005) 10–18.

[59] J.L. Fritz, M.J. Owen, Hydrophobic recovery of plasma-treated polydimethylsiloxane, J. Adhes. 54 (1–4) (1995) 33–45.

[60] H. Hillborg, U.W. Gedde, Hydrophobicity recovery of polydimethylsiloxane after exposure to corona discharges, Polymer 39 (10) (1998) 1991–1998.

[61] A. Tóth, I. Bertóti, M. Blazsó, G. Bánhegyi, A. Bognar, P. Szaplonczay, Oxidative damage and recovery of silicone rubber surfaces. I. X-ray photoelectron spectroscopic study, J. Appl. Polym. Sci. 52 (9) (1994) 1293–1307.

[62] M.J. Owen, P.J. Smith, Plasma treatment of polydimethylsiloxane, J. Adhes. Sci. Technol. 8 (10) (1994) 1063–1075.

[63] H.J. Hettlich, F. Otterbach, C.H. Mittermayer, R. Kaufmann, D. Klee, Plasma-induced surface modifications on suicone intraocular lenses: chemical analysis and in vitro characterization, Biomaterials 12 (5) (1991) 521–524.

[64] H. Hillborg, J.F. Ankner, U.W. Gedde, G.D. Smith, H.K. Yasuda, K. Wikström, Crosslinked polydimethylsiloxane exposed to oxygen plasma studied by neutron reflectometry and other surface specific techniques, Polymer 41 (18) (2000) 6851–6863.

[65] M.F. Meissner, Microfluidics on the Colloidal Scale (Ph.D. thesis), University of Bristol, 2017.

[66] D. Bodas, C. Khan-Malek, Hydrophilization and hydrophobic recovery of PDMS by oxygen plasma and chemical treatment—an SEM investigation, Sens. Actuators B 09254005, 123 (1) (2007) 368–373, https://doi. org/10.1016/j.snb.2006.08.037. http://linkinghub.elsevier.com/retrieve/pii/S0925400506006113.

[67] Y. Berdichevsky, J. Khandurina, A. Guttman, Y.-H. Lo, UV/ozone modification of poly(dimethylsiloxane) microfluidic channels, Sens. Actuators B 97 (2) (2004) 402–408.

[68] H.-Y. Chen, A.A. McClelland, Z. Chen, J. Lahann, Solventless adhesive bonding using reactive polymer coatings, Anal. Chem. 80 (11) (2008) 4119–4124.

[69] H. Makamba, Y.-Y. Hsieh, W.-C. Sung, S.-H. Chen, Stable permanently hydrophilic protein-resistant thin-film coatings on poly(dimethylsiloxane) substrates by electrostatic self-assembly and chemical cross-linking, Anal. Chem. 77 (13) (2005) 3971–3978.

[70] G. Mehta, M.J. Kiel, J.W. Lee, N. Kotov, J.J. Linderman, S. Takayama, Polyelectrolyte-clay-protein layer films on microfluidic PDMS bioreactor surfaces for primary murine bone marrow culture, Adv. Funct. Mater. 17 (15) (2007) 2701–2709.

[71] G.T. Roman, C.T. Culbertson, Surface engineering of poly(dimethylsiloxane) microfluidic devices using transition metal sol-gel chemistry, Langmuir 22 (9) (2006) 4445–4451.

[72] W.A.C. Bauer, M. Fischlechner, C. Abell, W.T.S. Huck, Hydrophilic PDMS microchannels for high-throughput formation of oil-in-water microdroplets and water-in-oil-in-water double emulsions, Lab Chip 1473-0197, 10 (14) (2010) 1814, https://doi.org/10.1039/c004046k. http://xlink.rsc.org/?DOI=c004046k.

[73] T. Trantidou, Y. Elani, E. Parsons, O. Ces, Hydrophilic surface modification of PDMS for droplet microfluidics using a simple, quick, and robust method via PVA deposition, Microsyst. Nanoeng. 3 (2017) 16091.

[74] D. Wu, Y. Luo, X. Zhou, Z. Dai, B. Lin, Multilayer poly(vinyl alcohol)-adsorbed coating on poly (dimethylsiloxane) microfluidic chips for biopolymer separation, Electrophoresis 26 (1) (2005) 211–218.

[75] T. Serizawa, S. Hashiguchi, M. Akashi, Stepwise assembly of ultrathin poly(vinyl alcohol) films on a gold substrate by repetitive adsorption/drying processes, Langmuir 15 (16) (1999) 5363–5368.

[76] G. Sui, J. Wang, C.-C. Lee, W. Lu, S.P. Lee, J.V. Leyton, A.M. Wu, H.-R. Tseng, Solution-phase surface modification in intact poly(dimethylsiloxane) microfluidic channels, Anal. Chem. 78 (15) (2006) 5543–5551.

[77] J.C. McDonald, G.M. Whitesides, Poly(dimethylsiloxane) as a material for fabricating microfluidic devices. Acc. Chem. Res 0001-4842, 35 (7) (2002) 491–499, https://doi.org/10.1021/ac001132d.

[78] R. Dangla, F. Gallaire, C.N. Baroud, Microchannel deformations due to solvent-induced PDMS swelling, Lab Chip 10 (21) (2010) 2972–2978.

[79] P. Wägli, A. Homsy, N.F. de Rooij, Norland optical adhesive (NOA81) microchannels with adjustable wetting behavior and high chemical resistance against a range of mid-infrared-transparent organic solvents, Sens. Actuators B 09254005, 156 (2) (2011) 994–1001, https://doi.org/10.1016/j.snb.2011.02.005. http://linkinghub. elsevier.com/retrieve/pii/S0925400511001031.

[80] S.H. Kim, Y. Yang, M. Kim, S.W. Nam, K.M. Lee, N.Y. Lee, Y.S. Kim, S. Park, Simple route to hydrophilic microfluidic chip fabrication using an ultraviolet (UV)-cured polymer, Adv. Funct. Mater. 1616301X, 17 (17) (2007) 3493–3498, https://doi.org/10.1002/adfm.200601203.

[81] D. Bartolo, G. Degré, P. Nghe, V. Studer, Microfluidic stickers, Lab Chip 1473-0197, 8 (2) (2008) 274–279, https://doi.org/10.1039/B712368J. http://xlink.rsc.org/?DOI=B712368J.

[82] C. Martino, J. Andrew, V.P. Weg, Droplet-based microfluidics for artificial cell generation: a brief review, Interface Focus 2042-8898, 6 (2016), https://doi.org/10.1098/rsfs.2016.0011.

[83] M.T. Guo, A. Rotem, J.A. Heyman, D.A. Weitz, Droplet microfluidics for high-throughput biological assays, Lab Chip 1473-0197, 12 (12) (2012) 2146, https://doi.org/10.1039/c2lc21147e.

[84] C. Yi, C.W. Li, S. Ji, M. Yang, Microfluidics technology for manipulation and analysis of biological cells, Anal. Chim. Acta 00032670560 (1-2) (2006) 1–23, https://doi.org/10.1016/j.aca.2005.12.037.

[85] E. Delamarche, D. Juncker, H. Schmid, Microfluidics for processing surfaces and miniaturizing biological assays. Adv. Mater. 0935964817 (24) (2005) 2911–2933, https://doi.org/10.1002/adma.200501129.

[86] T. Nisisako, T. Torii, T. Higuchi, Droplet formation in a microchannel network, Lab Chip 2 (1) (2002) 24–26.

[87] T. Nisisako, S. Okushima, T. Torii, Controlled formulation of monodisperse double emulsions in a multiple-phase microfluidic system, Soft Matter 1 (1) (2005) 23–27.

[88] M.F. Haase, J. Brujic, Tailoring of high-order multiple emulsions by the liquid-liquid phase separation of ternary mixtures, Angew. Chem. Int. Ed. 53 (44) (2014) 11793–11797.

[89] S.L. Anna, N. Bontoux, H.A. Stone, Formation of dispersions using "flow focusing" in microchannels, Appl. Phys. Lett. 00036951, 82 (3) (2003) 364–366, https://doi.org/10.1063/1.1537519.

[90] W.A.C. Bauer, J. Kotar, P. Cicuta, R.T. Woodward, J.V.M. Weaver, W.T.S. Huck, Microfluidic production of monodisperse functional o/w droplets and study of their reversible pH dependent aggregation behavior, Soft Matter 1744-683X, 7 (9) (2011) 4214, https://doi.org/10.1039/c1sm05087g.

[91] J. Don, M. Meissner, J. Eggers, A.M. Seddon, C.P. Royall, Opposed flow focusing: evidence of a second order jetting transition, arXiv preprint arXiv:1804.01471 (2018).

[92] C. Cohen, R. Giles, V. Sergeyeva, N. Mittal, P. Tabeling, D. Zerrouki, J. Baudry, J. Bibette, N. Bremond, Parallelised production of fine and calibrated emulsions by coupling flow-focusing technique and partial wetting phenomenon, Microfluid. Nanofluid. 16134982, 17 (2014) 959–966, https://doi.org/10.1007/s10404-014-1363-5.

[93] D.R. Link, S.L. Anna, D.A. Weitz, H.A. Stone, Geometrically mediated breakup of drops in microfluidic devices, Phys. Rev. Lett. 92 (5) (2004) 054503.

[94] W.-C. Jeong, J.-M. Lim, J.-H. Choi, J.-H. Kim, Y.-J. Lee, S.-H. Kim, G. Lee, J.-D. Kim, G.-R. Yi, S.-M. Yang, Controlled generation of submicron emulsion droplets via highly stable tip-streaming mode in microfluidic devices, Lab Chip 12 (8) (2012) 1446–1453.

[95] L. Rayleigh, On the instability of jets, Proc. Lond. Math. Soc. 1 (1) (1878) 4–13.

[96] T. Thorsen, R.W. Roberts, F.H. Arnold, S.R. Quake, Dynamic pattern formation in a vesicle-generating microfluidic device, Phys. Rev. Lett. 00319007, 86 (18) (2001) 4163–4166, https://doi.org/10.1103/PhysRevLett.86.4163.

[97] A.M. Gañán-Calvo, J.M. Gordillo, Perfectly monodisperse microbubbling by capillary flow focusing, Phys. Rev. Lett. 0031-9007, 87 (27, Pt 1) (2001) 274501, https://doi.org/10.1103/PhysRevLett.87.274501.

[98] S.L. Anna, Droplets and bubbles in microfluidic devices, Ann. Rev. Fluid Mech. 0066-4189, 48 (1) (2016) 285–309, https://doi.org/10.1146/annurev-fluid-122414-034425. http://www.annualreviews.org/doi/10.1146/annurev-fluid-122414-034425.

[99] G.F. Christopher, N.N. Noharuddin, J.A. Taylor, S.L. Anna, Experimental observations of the squeezing-to-dripping transition in T-shaped microfluidic junctions, Phys. Rev. E 78 (3) (2008) 036317.

[100] W. Lee, L.M. Walker, S.L. Anna, Role of geometry and fluid properties in droplet and thread formation processes in planar flow focusing, Phys. Fluids 10706631, 21 (3) (2009) 032103, https://doi.org/10.1063/1.3081407.

[101] B. Dollet, W. Van Hoeve, J.-P. Raven, P. Marmottant, M. Versluis, Role of the channel geometry on the bubble pinch-off in flow-focusing devices, Phys. Rev. Lett. 100 (3) (2008) 034504.

[102] P.J.A. Janssen, H.E.H. Meijer, P.D. Anderson, Stability and breakup of confined threads, Phys. Fluids 24 (1) (2012) 012102.

[103] P. Garstecki, H.A. Stone, G.M. Whitesides, Mechanism for flow-rate controlled breakup in confined geometries: a route to monodisperse emulsions, Phys. Rev. Lett. 0031-9007, 94 (16) (2005) 164501, https://doi.org/10.1103/PhysRevLett.94.164501.

[104] A.M. Gañán-Calvo, Unconditional jetting, Phys. Rev. E 78 (2) (2008) 026304.

[105] M.A. Herrada, A.M. Gañán-Calvo, A. Ojeda-Monge, B. Bluth, P. Riesco-Chueca, Liquid flow focused by a gas: jetting, dripping, and recirculation, Phys. Rev. E 78 (3) (2008) 036323.

[106] K.J. Humphry, A. Ajdari, A. Fernández-Nieves, H.A. Stone, D.A. Weitz, Suppression of instabilities in multiphase flow by geometric confinement, Phys. Rev. E 79 (5) (2009) 056310.

[107] A.S. Utada, A. Fernandez-Nieves, H.A. Stone, D.A. Weitz, Dripping to jetting transitions in coflowing liquid streams, Phys. Rev. Lett. 99 (9) (2007) 094502.

[108] D.R. Link, E. Grasland-Mongrain, A. Duri, F. Sarrazin, Z. Cheng, G. Cristobal, M. Marquez, D. A. Weitz, Electric control of droplets in microfluidic devices, Angew. Chem. Int. Ed. 45 (16) (2006) 2556–2560.

[109] N.-T. Nguyen, T.-H. Ting, Y.-F. Yap, T.-N. Wong, J.C.-K. Chai, W.-L. Ong, J. Zhou, S.-H. Tan, L. Yobas, Thermally mediated droplet formation in microchannels, Appl. Phys. Lett. 91 (8) (2007) 084102.

[110] S.-Y. Park, T.-H. Wu, Y. Chen, M.A. Teitell, P.-Y. Chiou, High-speed droplet generation on demand driven by pulse laser-induced cavitation, Lab Chip 11 (6) (2011) 1010–1012.

[111] C. Rivet, H. Lee, A. Hirsch, S. Hamilton, H. Lu, Microfluidics for medical diagnostics and biosensors, Chem. Eng. Sci. 66 (7) (2011) 1490–1507.

[112] Y. Schaerli, R.C. Wootton, T. Robinson, V. Stein, C. Dunsby, M.A.A. Neil, P.M.W. French, A. J. DeMello, C. Abell, F. Hollfelder, Continuous-flow polymerase chain reaction of single-copy DNA in microfluidic microdroplets, Anal. Chem. 81 (1) (2008) 302–306.

[113] J.-C. Baret, O.J. Miller, V. Taly, M. Ryckelynck, A. El-Harrak, L. Frenz, C. Rick, M.L. Samuels, J. B. Hutchison, J.J. Agresti, Fluorescence-activated droplet sorting (FADS): efficient microfluidic cell sorting based on enzymatic activity, Lab Chip 9 (13) (2009) 1850–1858.

[114] N. Bremond, A.R. Thiam, J. Bibette, Decompressing emulsion droplets favors coalescence, Phys. Rev. Lett. 100 (2) (2008) 024501.

[115] B. Abecassis, C. Cottin-Bizonne, C. Ybert, A. Ajdari, L. Bocquet, Boosting migration of large particles by solute contrasts, Nat. Mater. 7 (10) (2008) 785–789.

[116] K.N. Nordstrom, E. Verneuil, P.E. Arratia, A. Basu, Z. Zhang, A.G. Yodh, J.P. Gollub, D. J. Durian, Microfluidic rheology of soft colloids above and below jamming, Phys. Rev. Lett. 105 (17) (2010) 175701.

[117] E. Um, D.-S. Lee, H.-B. Pyo, J.-K. Park, Continuous generation of hydrogel beads and encapsulation of biological materials using a microfluidic droplet-merging channel, Microfluid. Nanofluid. 5 (4) (2008) 541–549.

[118] Z. Nie, W. Li, M. Seo, S. Xu, E. Kumacheva, Janus and ternary particles generated by microfluidic synthesis: design, synthesis, and self-assembly, J. Am. Chem. Soc. 128 (29) (2006) 9408–9412.

[119] B. Shen, J. Ricouvier, F. Malloggi, P. Tabeling, Designing Colloidal Molecules with Microfluidics, Adv. Sci. 3 (6) (2016) 1600012.